

A Fast and Effective Method for Euclidean Anticlustering: The Assignment-Based-Anticlustering Algorithm

P. Baumann^{*1}, O. Goldschmidt², D. S. Hochbaum³, and J. Yang³

¹Department of Business Administration, University of Bern, Engehaldenstr. 4, 3012 Bern, Switzerland

²Riverside County Office of Education, Riverside, CA 92501, USA

³Industrial Engineering and Operations Research Department, University of California, Berkeley, CA 94720, USA

philipp.baumann@unibe.ch, goldoliv@gmail.com, dhochbaum@berkeley.edu, jason_yang@berkeley.edu

Abstract

The anticlustering problem is to partition a set of objects into K equal-sized antoclusters, such that the sum of distances, or dissimilarities, within antoclusters is maximized. In that each antocluster reflects the diversity of the entire set of objects. The anticlustering problem is NP-hard. We focus on anticlustering in Euclidean spaces, where the input data is tabular with each object represented as a D -dimensional feature vector. The dissimilarities or distances are measured as squared Euclidean distances between the respective vectors. Applications of Euclidean anticlustering include social studies, particularly in the field of psychology, K -fold cross-validation in which the goal is for each of the K folds to be a good representative of the entire dataset, creating mini-batches for stochastic gradient descent in neural network training, and finding balanced K -cut partitions. In particular, machine-learning applications such as mini-batch generation involve million-scale datasets and very large values of K , making scalable anticlustering algorithms essential. Existing algorithms are either exact algorithms that are only capable of solving small-sized instances, up to 100 objects, or heuristic algorithms among which the most scalable algorithm is an exchange-based heuristic called `fast_anticlustering`. We propose here a new algorithm, the *Assignment-Based Anticlustering* algorithm (ABA) that scales to very large instances. In a computational study, it is shown that ABA outperforms `fast_anticlustering` in both solution quality and running time. Furthermore, ABA scales to instances with millions of objects and hundreds of thousands of antoclusters within reasonable running times, which is beyond what `fast_anticlustering` can manage. As a balanced K -cut partitioning method for tabular data, ABA is shown in the experimental study to be far superior to the well-known METIS method, both in solution quality and running time. We also present an adaptation of ABA to *anticlustering with categories*, where objects from each category must be equally represented in every antocluster. In this setting, ABA again achieves superior results compared to the known methods of `fast_anticlustering` and a recent integer linear programming model. The code of the ABA algorithm is available at [GitHub](https://github.com/phil85/aba)¹.

1 Introduction

Anticlustering is an NP-hard combinatorial optimization problem that consists of partitioning a set of objects into equally-sized groups called antoclusters such that the objects in the same antocluster are as diverse as possible and thereby representative of the entire set of objects. Achieving diversity within groups is important in many applications from various fields including operations research (Weitz and Lakshminarayanan 1997, Baker and Powell 2002, Palubeckis et al. 2015, Lai and Hao 2016, Schulz 2021, 2023a,b, Hochbaum et al. 2023), management science (Krass and Ovchinnikov 2006), psychology and social sciences (Brusco et al. 2020, Papenberg and Klau 2021), bioinformatics (Papenberg et al. 2025b), VLSI circuit design (Chen 1986, Feo and Khellaf 1990), computer systems and memory management (Kral 1965), and more recently machine learning (Mauri et al. 2023).

^{*}Corresponding author: philipp.baumann@unibe.ch

¹<https://github.com/phil85/aba>

Several antoclustering variants have been proposed in the literature that differ in how the objects are represented, how diversity is measured, which objective is optimized, and which additional constraints are considered. Antoclustering is also studied under the name maximally diverse grouping problem (MDGP), see Gallego et al. 2013. We focus here on antoclustering in Euclidean spaces, where objects are represented as feature vectors and diversity is measured using squared Euclidean distances. The objective is to assign an equal number of objects to each antocluster so that the sum of pairwise squared Euclidean distances between objects within antoclusters is maximized. Euclidean antoclustering can be traced back to Späth [1986] and is now arguably the most widely-used variant of antoclustering in practice. In psychology and social sciences, it is used to create participant groups that are comparable and representative of the entire dataset (Papenberg and Klau 2021). In biomedical research such as high-throughput sequencing, it is used to assign patient DNA and RNA samples to batches to limit batch effects (see Papenberg et al. 2025b). In unsupervised learning, it is used to split datasets into diverse subsets to help compute lower bounds for instances of the minimum sum-of-squares clustering problem (see Croella et al. [2025]). In supervised learning, it is used in cross-validation to create representative folds that support reliable model evaluation (see Papenberg and Klau 2021), and in neural network training to form mini-batches for stochastic gradient descent, improving model generalization and convergence (see Joseph et al. 2019, Wang et al. 2019, Banerjee and Chakraborty 2021). These recent applications in machine learning involve very large instances of Euclidean antoclustering with millions of objects and thousands of antoclusters. Although antoclustering is often considered easier on large datasets because random partitions are more likely to produce reasonable solutions, this effect mainly holds when the number of antoclusters is small. In applications such as mini-batch generation for neural network training, however, a large number of antoclusters is required. In such settings, Euclidean antoclustering remains challenging, creating a strong demand for scalable antoclustering algorithms.

Various exact and heuristic methods have been developed for antoclustering. Exact methods are primarily based on mixed-integer programming formulations and are limited to small instances, solving problems with up to about 100 objects [Gallego et al., 2013, Papenberg and Klau, 2021]. For special cases using Manhattan distances, moderately larger instances with a few hundred objects can be solved [Schulz, 2021, 2022, 2023b], and when feature values are integer, instances with up to several thousand objects become tractable [Schulz, 2023a]. For larger instances, numerous heuristics have been introduced. Feo et al. [1992] propose approximation algorithms for instances in which antoclusters contain exactly three or four objects. These algorithms run in cubic time in the number of objects and are therefore not suitable for large-scale applications. The heuristics developed for the MDGP work with a complete distance matrix, which limits their scalability (see Palubeckis et al. 2015, Lai and Hao 2016, Singh and Sundar 2019, Yang et al. 2022). Other heuristics developed for antoclustering are typically exchange-based. They start from a random partition and iteratively improve it by exchanging pairs of objects from different antoclusters. This strategy does not require the complete distance matrix and is therefore more scalable. However, when the number of desired antoclusters K is large, a substantial number of exchanges may be required to achieve high-quality solutions, which can lead to large running times. These exchange-based heuristics as well as the heuristic of Yang et al. [2022] for the MDGP have been implemented in the R package called **anticlust** (see Papenberg and Klau 2021). The package also includes an exchange-based heuristic called **fast_antoclustering**, which was the most scalable heuristic available for Euclidean antoclustering to date. It works in the same way as the standard exchange-based heuristic, but considers only a user-defined number of exchange partners for each object and uses a different formulation of the objective function which allows for substantially faster evaluation. However, the fast-antoclustering method is also exchange-based, which means that the quality of the solution depends on the number of exchange partners considered for each object. As we will see in the computational analysis, for instances with millions of objects, thousands of features, and tens of thousands of antoclusters, the method fails to find solutions, or requires a large number of exchange partners to achieve high-quality results, which leads to high running time. Such large-scale instances arise in machine learning applications such as the construction of mini-batches for stochastic gradient descent in neural network training. In this setting, objects typically correspond to images represented by high-dimensional feature vectors, and a large number of mini-batches is required for effective training. The methods available in the **anticlust** package are not capable of solving such large instances within reasonable running times. For such instances, greedy constructive methods have been proposed (see Joseph et al. 2019, Wang et al. 2019, Banerjee and Chakraborty 2021). These methods generate mini-batches that enable faster convergence and higher neural network accuracy, however, they remain computationally expensive, requiring hours of running time for processing standard image datasets such as ImageNet. In addition to the limited scalability of available methods, another limitation is that they do not ensure that the antoclusters are similar to each other in terms of diversity. As pointed out by Schulz [2021] and Papenberg [2024], in many applications, it is not only important to achieve high diversity within each antocluster, but also to ensure that the antoclusters are similar to each other in terms of diversity.

In this paper, we address the limitations of existing methods by introducing a novel heuristic, the Assignment-Based Anticlustering (ABA) algorithm. The ABA algorithm is a constructive heuristic that builds a solution with a single pass over the objects, avoiding the need for iterative improvement procedures. It solves a sequence of assignment problems that assign batches of objects to antoclusters. The antoclusters are represented by centroids, and distances are computed only between objects and centroids, rather than between pairs of objects. This substantially improves scalability. After each batch assignment, the centroids of antoclusters are updated. The batches are formed based on the distances of objects to the global centroid of the dataset, ensuring that objects of similar centrality are distributed evenly across antoclusters. This leads to antoclusters with similar levels of diversity. We also introduce a hierarchical decomposition strategy that further improves the scalability of our approach and offers the possibility to leverage parallel computation.

In a comprehensive computational analysis, we demonstrate that the ABA algorithm outperforms leading anticlustering methods in both solution quality and running time. Moreover, the ABA algorithm produces antoclusters which are considerably more similar to each other in terms of diversity than the antoclusters produced with other methods. The ABA algorithm scales to very large instances with millions of objects and thousands of antoclusters within seconds to minutes. We also demonstrate the versatility of the ABA algorithm by showing how it can be adapted to related problems. For example, we show that ABA can be effectively applied to balanced K -cut partitioning of tabular data, achieving superior results compared to the well-known METIS method in terms of both solution quality and running time. Furthermore, we present an adaptation of ABA to anticlustering with categories, where objects from each category must be equally represented in every antocluster. In this setting, ABA again achieves superior results compared to the known methods of `fast_anticlustering` and the recent integer linear programming model of Croella et al. [2025].

The remainder of the paper is organized as follows. Section 2 formalizes the anticlustering problem and introduces the notation used throughout. Section 3 reviews existing algorithms for Euclidean anticlustering and related problems and identifies the research gaps that motivate our work. Section 4 presents the Assignment-Based Anticlustering (ABA) algorithm, including its base version, extensions for small antoclusters and categorical balancing, a hierarchical speed-up, and a runtime analysis. Section 5 reports our experimental results, covering datasets, benchmark methods, comparisons on standard and categorical anticlustering tasks, and applications to balanced K -cut. Section 6 concludes and outlines future research directions.

2 Problem Description

Let $G = (V, E)$ be an undirected, weighted graph with $V = \{1, \dots, N\}$ the set of nodes (objects), $E \subseteq \{\{i, j\} : i < j, i, j \in V\}$ the set of edges, and edge weights $w_{ij} \geq 0$ representing dissimilarities between nodes i and j . The anticlustering problem consists of partitioning the set of nodes into K groups (antoclusters) of equal size such that the sum of pairwise dissimilarities (or edge weights) within each group is maximized (see Späth 1986). The problem is NP-hard because even the case of partitioning into two equally sized groups is at least as hard as the balanced cut problem (see Garey and Johnson 1990). In this work, we focus on the most common variant, where objects are points in a D -dimensional Euclidean space and pairwise dissimilarities are defined by squared Euclidean distances.

Formally, the problem we study can be described as follows. Given is a dataset $\mathcal{X} = \{\mathbf{x}_1, \dots, \mathbf{x}_N\}$ with N objects and D features, in which $\mathbf{x}_i = [x_{i1}, \dots, x_{iD}] \in \mathbb{R}^D$ is the i -th object, x_{id} is the d -th feature of the i -th object, and $\mathcal{N} := \{1, \dots, N\}$ is the set of object indices. The objective is to find a partition $\mathcal{C} = \{\mathcal{C}_1, \dots, \mathcal{C}_K\}$ of the objects into K antoclusters of “approximately” equal size such that the total sum of squared Euclidean distances between objects within the same antocluster is maximized. Here we interpret “approximately” equal size, as sizes that are strictly less than one unit away from the average size (N/K). Let $\mathcal{K} := \{1, \dots, K\}$ denote the set of antocluster indices, \mathcal{C}_k the set of object indices in antocluster k , and $d(i, i') = \|\mathbf{x}_i - \mathbf{x}_{i'}\|_2^2$ the squared Euclidean distance between objects i and i' . With this notation, the anticlustering problem in Euclidean space can be formulated as follows:

$$\left\{ \begin{array}{ll} \max_{\mathcal{C} = \{\mathcal{C}_1, \dots, \mathcal{C}_K\}} & W(\mathcal{C}) = \sum_{k \in \mathcal{K}} \sum_{i, i' \in \mathcal{C}_k, i < i'} d(i, i') \\ \text{(Euclidean anticlustering)} & \text{s.t. } \lfloor N/K \rfloor \leq |\mathcal{C}_k| \leq \lceil N/K \rceil \quad (k \in \mathcal{K}) \quad (2) \\ & \bigcup_{k \in \mathcal{K}} \mathcal{C}_k = \mathcal{N} \quad (3) \\ & \mathcal{C}_k \cap \mathcal{C}_{k'} = \emptyset \quad (k, k' \in \mathcal{K}, k < k') \quad (4) \end{array} \right.$$

The objective function computes the sum of pairwise squared Euclidean distances between objects assigned

Notation	Description
N	Number of objects
\mathcal{N}	Set of object indices
\mathcal{N}_g	Set of indices of objects belonging to category g
N_k	Number of objects in antocluster k
D	Number of features
K	Number of antoclusters
$\mathcal{K} = \{1, \dots, K\}$	Set of antocluster indices
$\mathcal{G} = \{1, \dots, G\}$	Set of categories
G	Number of categories
$\mathcal{C} = \{\mathcal{C}_1, \dots, \mathcal{C}_K\}$	Set of antoclusters (partition)
\mathcal{C}_k	Set of object indices in antocluster k
$W(\mathcal{C})$	Within-cluster sum of squared distances of partition \mathcal{C}
$\mathcal{X} = \{\mathbf{x}_1, \dots, \mathbf{x}_N\}$	Dataset
$\mathbf{x}_i = [x_{i1}, \dots, x_{iD}]$	Object i
x_{id}	d -th feature of object i
$\boldsymbol{\mu}$	Global centroid of the dataset
$\boldsymbol{\mu}_k$	Centroid of antocluster k
\mathcal{N}^\downarrow	List of object indices sorted by decreasing distance $d(i, \boldsymbol{\mu})$
$d(i, i')$	Squared Euclidean distance between object x_i and $x_{i'}$

Table 1: Notation used in the paper

to the same antocluster. Constraints (2) ensure that the size of two antoclusters differs by at most one object. Constraints (3) and (4) ensure that every object is assigned to exactly one antocluster.

We also consider an extension of the antoclustering problem in Euclidean space where each object is associated with a category g from a given set of categories $\mathcal{G} = \{1, \dots, G\}$. Let $\mathcal{N}_g := \{i \in \mathcal{N} \mid \text{category}(i) = g\}$ be the indices of the objects that belong to category $g \in \mathcal{G}$. With this additional notation, the antoclustering problem in Euclidean space with categories can be formulated as follows:

$$(\text{Euclidean antoclustering with categories}) \left\{ \begin{array}{l} \max_{\mathcal{C}=\{\mathcal{C}_1, \dots, \mathcal{C}_K\}} W(\mathcal{C}) \\ \text{s.t.} \quad (2), (3), (4) \\ \quad \left\lfloor \frac{|\mathcal{N}_g|}{K} \right\rfloor \leq |\mathcal{C}_k \cap \mathcal{N}_g| \leq \left\lceil \frac{|\mathcal{N}_g|}{K} \right\rceil \quad (k \in \mathcal{K}, g \in \mathcal{G}) \end{array} \right. \quad (5)$$

In this extended formulation, constraints (5) ensure that for each category $g \in \mathcal{G}$, the number of objects belonging to category g differs by at most one between each pair of antoclusters. Specifically, the number of objects from category g assigned to any antocluster \mathcal{C}_k is constrained to lie between $\lfloor |\mathcal{N}_g|/K \rfloor$ and $\lceil |\mathcal{N}_g|/K \rceil$, so that all antoclusters reflect the overall category distribution. A summary of the notation that is used throughout the paper can be found in Table 1.

3 Literature review

In this section, we review existing algorithms that can be applied to Euclidean antoclustering or closely related problems. Section 3.1 discusses exact approaches and Section 3.2 reviews heuristic approaches. Finally, Section 3.3 discusses the limitations of existing algorithms and identifies the research gaps addressed in this paper.

3.1 Exact approaches

To the best of our knowledge, no exact algorithm has been developed specifically for Euclidean antoclustering. However, exact methods for the maximally diverse grouping problem (MDGP) can be applied to Euclidean antoclustering. The MDGP is defined on an undirected complete graph $G = (V, E)$ with nonnegative edge weights w_{ij} representing pairwise dissimilarities between nodes i and j . The objective is to partition the node set V into K

groups of bounded size such that the sum of pairwise dissimilarities within each group is maximized. Euclidean antoclustering can be formulated as an instance of the MDGP by using squared Euclidean distances as edge weights and enforcing equal group sizes through appropriate bounds. Since the MDGP is NP-hard, only a few exact approaches have been proposed.

Gallego et al. [2013] present a standard integer linear programming formulation of the MDGP, which can be used as an exact solution approach in combination with a general-purpose solver. An alternative formulation for the MDGP with equal-sized groups was introduced by Papenberg and Klau [2021], building on the work of Grötschel and Wakabayashi [1989].

Schulz [2021] study a special case of the MDGP in which dissimilarities are measured using the Manhattan distance and all groups must be of equal size. They show that the set of optimal solutions can be characterized by a system of constraints that includes so-called block constraints. Since the number of optimal solutions may be very large, they propose an objective function that aims to balance diversity across groups. An exact approach that is based on the system of constraints and the new objective function is presented. In a follow-up study, Schulz [2022] compare a variant of this exact approach to the formulations of Gallego et al. [2013] and Papenberg and Klau [2021] and find that it performs best for the Manhattan-distance setting. Schulz [2023b] extend this work and propose a two-step exact mixed-integer programming approach, reporting optimal solutions for instances with up to 200 objects. Furthermore, Schulz [2023a] prove that, when feature values are integers, the considered special case can be solved in pseudo-polynomial time. They introduce both a dynamic programming approach and a mixed-integer programming formulation, with the latter solving instances with up to 6,000 objects to optimality within reasonable computation times.

Papenberg et al. [2025a] propose an exact approach for antoclustering with maximum dispersion, i.e., antoclustering with the goal of maximizing the minimum distance between any two objects within the same antocluster (see Brusco et al. 2020). Their method iteratively increases a distance threshold δ and, for each value, constructs a graph in which edges connect pairs of objects whose distance is below δ . A graph coloring integer program is solved to test K -colorability; the largest feasible δ yields the optimal maximum dispersion. Instances with up to 1,000 objects are solved to optimality. The same authors also develop an exact approach for bicriterion antoclustering, i.e., antoclustering with two different diversity criteria, namely the diversity and maximum dispersion (Brusco et al. 2020). After determining the optimal maximum dispersion, they solve the formulation of Papenberg and Klau [2021] using a modified distance matrix. Computational results show that this approach is practical only for small instances (up to 30 objects), motivating the development of hybrid methods that combine the exact dispersion approach with heuristics. Among these, an adaptation of the algorithm by Brusco et al. [2020] performs best.

3.2 Heuristic approaches

Only few heuristics have been specifically developed for Euclidean antoclustering, therefore in this section we also review heuristics that have been developed for related antoclustering problems.

Späth [1986] introduced Euclidean antoclustering and proposed a heuristic for the problem without antocluster-size constraints. The heuristic starts from a random partition of the objects and iteratively improves the solution by moving objects from one antocluster to another. For each object, the heuristic evaluates the improvement in the objective function that would result from moving the object to each of the other antoclusters and performs the move that yields the largest improvement. The process is repeated until no further improvement is possible. Weitz and Lakshminarayanan [1997] proposed a heuristic for antoclustering with cardinality constraints that considers pairwise exchanges of objects between antoclusters instead of single-object moves. The exchange-based heuristic works in the same way as the move-based heuristic, but instead of evaluating the improvement resulting from moving a single object, it evaluates the improvement resulting from exchanging pairs of objects from different antoclusters. The exchange that yields the largest improvement is performed. The process is repeated until no further improvement is possible.

In addition to the exact approach described in the previous section, Papenberg and Klau [2021] also presents a heuristic approach antoclustering. The heuristic is based on exchanging objects between antoclusters and is in that similar to the heuristics introduced by Späth [1986] and Brusco et al. [2020]. The heuristic begins with a random assignment of objects to antoclusters, ensuring that all antoclusters have equal size. It then selects an object and evaluates all pairwise exchanges between the selected object and objects from other antoclusters. The exchange that achieves the largest improvement in the objective value is performed. No exchange is performed if none improve the objective. The heuristic stops when the exchange process has been repeated for each object. The methods introduced in Papenberg and Klau [2021] are implemented in an R package called `anticlust`. This package also contains an implementation of the iterated local search approach of Brusco et al. [2020] and provides additional variants of the exchange-based heuristic of Papenberg and Klau [2021] including one called `fast-anticlustering`.

that is specifically designed for large instances of Euclidean antclustering. It works in the same way as the standard exchange-based heuristic, but considers only a user-defined number of exchange partners for each object and uses a different formulation of the objective function which allows for substantially faster evaluation. The default behaviour of `fast-anticlustering` is to generate exchange partners by using a nearest neighbor search. Using more exchange partners tends to improve the quality of the solution, but increases running time. To avoid running the nearest neighbor search, the exchange partners can be chosen randomly. An advantage of the exchange-based heuristic of Papenberg and Klau [2021] is that additional constraints can easily be integrated into the exchange process. This allows the heuristic to be applied to Euclidean antclustering with categories (see Section 2), and antclustering with must-link and cannot-link constraints between pairs of objects.

Numerous heuristics have been developed for antclustering under the name maximally diverse grouping problem (MDGP). These include, Palubeckis et al. [2015], Lai and Hao [2016], Lai et al. [2021], Singh and Sundar [2019], Yang et al. [2022]). The approach of Yang et al. [2022] has been included in a later version of the R package `anticlust`. It is a population-based metaheuristic that starts from an initial population of randomly generated solutions and iteratively applies three phases to evolve the population toward better solutions. Schulz [2023b] present in addition to the two-step exact mixed-integer programming approach mentioned in Section 3.1 also several heuristics for MDGP with Manhattan distance, i.e., the problem considered in Schulz [2021]. The approaches developed for the MDGP or special cases of it are limited in terms of scalability as they require to compute and store all pairwise distances between objects. This makes them less suitable for large instances of Euclidean antclustering where the number of objects is in the order of hundreds of thousands or millions.

Other types of antclustering heuristics have been developed in the context of mini-batch construction for machine learning. Wang et al. [2019] propose a method to generate representative, equal-size mini-batches for training neural networks. Their approach uses a greedy algorithm that starts with empty mini-batches and iteratively selects the least representative one. From the set of unassigned data points, the algorithm assigns the point that improves the representativeness of the selected mini-batch the most, repeating this process until all mini-batches reach the desired size. Representativeness is measured using a submodular function that evaluates how well the samples in a mini-batch represent the entire dataset, by summing, for each data point, the similarity to its most similar sample in the mini-batch. The authors further introduce a hierarchical variant of the algorithm to reduce memory and computational costs, and show on CIFAR-100 and ImageNet that the resulting mini-batch sequences consistently outperform random shuffling. However, the overall running time of the approach is dominated by the cost of constructing the similarity graph used by the submodular function. Even with class-wise sparsification, building this graph is expensive: the authors report approximately 3 minutes for CIFAR-100 and almost 90 minutes for ImageNet on a 16-core CPU, before any partitioning is performed.

Banerjee and Chakraborty [2021] propose a method for generating mini-batches sequentially. Mini-batches are constructed one at a time by solving an optimization problem that takes into account the objects already assigned to earlier mini-batches and those that have not yet been assigned. The goal of the optimization is to make the union of the earlier mini-batches together with the newly formed one representative of the not yet assigned objects. Representativeness is measured using the Maximum Mean Discrepancy, which compares the distributions of the selected and unselected objects through pairwise similarities computed by a kernel function. This leads to a formulation of the mini-batch selection problem as a constrained optimization problem with a fixed batch size, resulting in an NP-hard integer quadratic program. To make the approach tractable, the authors derive a linear programming relaxation and recover an integral solution via rounding. The approach is computationally expensive, since evaluating the MMD requires computing a kernel matrix containing pairwise similarities between all objects, and because the resulting linear program must be solved repeatedly for each mini-batch.

The antclustering problem was addressed as a bi-criterion problem combining diversity and maximum dispersion objectives. The diversity objective is to maximize the sum of pairwise distances within antoclusters and the maximum dispersion objective is to maximize the minimum distance between any two objects within the same antocluster. Brusco et al. [2020] were the first to address this bi-criterion antclustering problem. They extended the approach of Späth [1986] by using an exchange-based heuristic that seeks to maximize a weighted sum of the two objectives. The heuristic starts from a random partition and iteratively improves it by exchanging pairs of objects from different antoclusters. To approximate the Pareto efficient set of solutions, the heuristic is restarted multiple times, each time with different weights for two diversity criteria. Whenever a new solution is generated during any of the restarts, the Pareto efficient set is updated. Furthermore, the exchange-based heuristic is integrated into an iterated local search approach. Papenberg et al. [2025a] recently studied the bi-criterion antclustering problem. In addition to an exact approach, they propose hybrid methods that combine the exact dispersion computation with heuristics that optimize the diversity objective for a given level of maximum dispersion. Computational results show that among the hybrid methods an adaptation of the heuristic by Brusco et al. [2020] achieves the best performance.

3.3 Research gaps

We have identified several limitations of previous approaches that became the motivation for developing a new procedure to tackle the Euclidean antoclustering problem:

- Limited control over similarity between antoclusters: Papenberg [2024] mention a key limitation of existing algorithms for Euclidean antoclustering. Algorithms that maximize the sum of squared Euclidean distances within antoclusters, enforce similarity between antoclusters at the level of their centroids, that is, they align the means of the feature values. However, they do not target other distributional characteristics, such as the variance of feature values within antoclusters. As a result, antoclusters may exhibit similar means but differ significantly in terms of variance and other higher moments of the feature value distributions. In many applications, however, similarity between antoclusters is desired not only with respect to centroids, but also higher moments of feature value distributions. To overcome this limitation, Papenberg [2024] propose a data augmentation technique that allows to consider also higher moments of the feature value distributions. The idea is to add additional features to the dataset: for each original feature and for each moment to be addressed, a corresponding new feature is added. For example, to address the second moment (variance), a new feature is added for each original feature defined as the squared difference between the original feature value and the mean of that feature in the dataset. This strategy, however, increases the dimensionality of the data and may lead to high computational costs, especially when many moments are to be considered.
- Limited scalability: as demonstrated by computational studies in several papers, existing exact approaches are only applicable to small instances. Existing heuristics work with the complete pairwise distance matrix between objects or they consider pairwise exchanges between objects. This limits their scalability to large instances of Euclidean antoclustering where the number of objects is in the order of hundreds of thousands or millions.
- Lack of specialization: Although Euclidean antoclustering is the most prevalent variant in practical applications, only one heuristic has been specifically tailored to this setting, namely the **fast-antoclustering** method of Papenberg and Klau [2021]. However, the **fast-antoclustering** method is also exchange-based, which means that the quality of the solution depends on the number of exchange partners considered for each object. As we will see in the computational analysis, for instances with large N (number of objects), large D (number of features), and large K (number of antoclusters), the method fails to find solutions, or requires a large number of exchange partners to achieve high-quality results, which leads to high running time.

4 The New Assignment-Based Antoclustering (ABA) Algorithm

The ABA algorithm constructs an antoclustering solution by iteratively solving assignment problems. In each iteration, it selects a subset of objects and assigns it to antoclusters such that the total squared Euclidean distance between the objects and the centroids of the antoclusters is maximized. The centroids of the antoclusters are then updated based on the new assignments. With increasing iterations, this strategy tends to move the centroids toward the global centroid of the data, i.e., the mean of the data. A key idea is to form the subsets of objects based on their decreasing distance to the global centroid of the data, i.e., the first subset contains the objects furthest from the global centroid, the second subset contains those that are next furthest, and so on. Since the final positions of the antocluster centroids tend to be close to the global centroid, the proposed subset selection strategy ensures that each antocluster will have a similar distribution of distances between objects and the antocluster centroid. By representing antoclusters through their centroids, the ABA algorithm takes advantage of the equivalence between maximizing the within-cluster sum of squares and the within-cluster variance (see Fact 1). This allows distances to be computed between objects and centroids rather than between pairs of objects, resulting in greater computational efficiency. The following well-known fact establishes the equivalence between the sum of distances to the centroids of the respective antoclusters to the sum of squares of distances within the antoclusters. For completeness sake a proof of the fact is provided in the appendix.

Fact 1. For antocluster \mathcal{C}_k and centroid $\boldsymbol{\mu}_k = \frac{1}{|\mathcal{C}_k|} \sum_{i \in \mathcal{C}_k} \mathbf{x}_i$:

$$\sum_{i, i' \in \mathcal{C}_k, i < i'} \|\mathbf{x}_i - \mathbf{x}_{i'}\|_2^2 = |\mathcal{C}_k| \sum_{i \in \mathcal{C}_k} \|\mathbf{x}_i - \boldsymbol{\mu}_k\|_2^2.$$

In Section 4.1, we first describe the base version of the algorithm. In Section 4.2, we present a version of ABA that is tailored to small antoclusters and in Section 4.3, we introduce a version of the ABA algorithm that

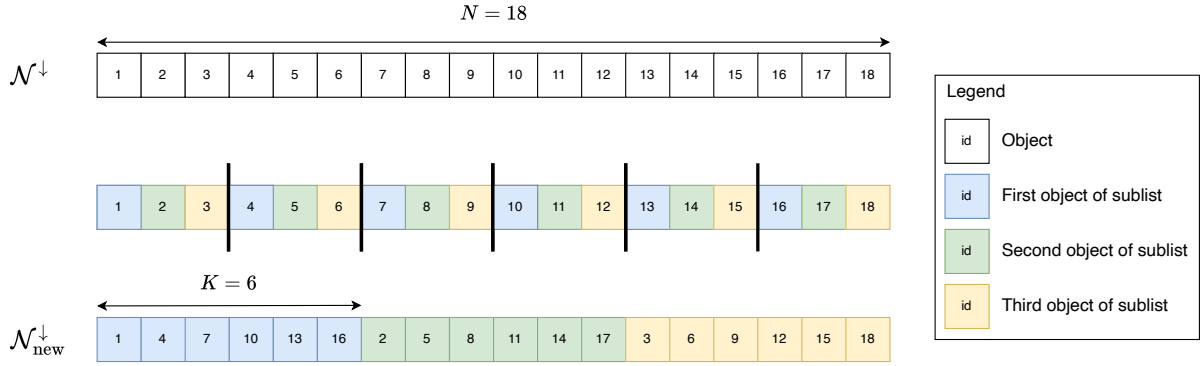


Figure 1: Illustration of how to rearrange the sorted list \mathcal{N}^\downarrow when N is divisible by K based on an example with $N = 18$ objects and $K = 6$ antoclusters

can be applied to the antoclustering problem in Euclidean space with categories (see Section 2). In Section 4.4, we present an acceleration technique that substantially speeds up the ABA algorithm, in particular when K is large. Finally, in Section 4.5, we discuss the running time complexity of the ABA algorithm.

4.1 Base Version of the ABA Algorithm

Algorithm 1 provides the pseudocode of the ABA algorithm and Table 1 describes the notation used. The ABA algorithm takes as input a dataset $\mathcal{X} = \{\mathbf{x}_1, \dots, \mathbf{x}_N\}$ consisting of N objects, each represented by a D -dimensional feature vector, and a parameter K which specifies the desired number of antoclusters. The algorithm starts by computing the squared Euclidean distances between each object \mathbf{x}_i with $i = 1, \dots, N$ and the centroid of the dataset $\boldsymbol{\mu} = \frac{1}{N} \sum_{i=1, \dots, N} \mathbf{x}_i$. The algorithm then creates a list \mathcal{N}^\downarrow which contains the indices of the objects, sorted by their distance to the global centroid $\boldsymbol{\mu}$ in descending order. The list \mathcal{N}^\downarrow is split into $B = \lceil N/K \rceil$ batches. The first batch \mathcal{B}_1 contains the first K indices of \mathcal{N}^\downarrow , the batch \mathcal{B}_2 the next K , and so on. Thus, all batches contain K indices, with the possible exception of the last batch \mathcal{B}_B if N is not divisible by K . Next, the algorithm assigns each object whose index is contained in \mathcal{B}_1 to one of the K antoclusters and initializes the centroid of each antocluster with the feature vector of its assigned object. The remaining $B - 1$ batches are processed as follows. Given a batch \mathcal{B}_i , a cost matrix of size $|\mathcal{B}_i| \times K$ is computed where each entry j, k $j = 1, \dots, |\mathcal{B}_i|$ and $k = 1, \dots, K$ corresponds to the squared Euclidean distance between the corresponding object $\mathbf{x}_{\mathcal{B}_i[j]}$ and the corresponding centroid of antocluster $\boldsymbol{\mu}_k$. The cost matrix is passed to a linear assignment problem solver that determines the maximal cost assignment. Based on the new assignments, the centroids of the antoclusters are updated. After the processing of all batches, the ABA algorithm returns a vector of length N that contains for each object the label of the antocluster to which it was assigned.

4.2 The ABA Algorithm for Small Antoclusters

Empirically, we found that a variant on forming the batches generally outperforms the one described above for small antoclusters. We therefore propose a variant of ABA that is tailored to instances with small antoclusters. The main idea of this variant is to rearrange the objects in the sorted list \mathcal{N}^\downarrow such that the selection of objects in the batches is more diverse in terms of distances to the global centroid. Unlike the base version of the ABA procedure, described above, that has each batch containing objects of similar and lesser distances than the previous batch, we aim to diversify the distances within the batches so that each batch contains a representation from high to low distances. The adjustment is done as follows.

If N is divisible by K , we divide the sorted list \mathcal{N}^\downarrow into K sublists, each of length $Q = N/K$. We rearrange the order of the objects in list \mathcal{N}^\downarrow by repeatedly taking the first/next object from each sublist in order: initially the first object from each sublist, then the second object from each sublist, and so on. This continues until all N objects have been processed. The algorithm then continues with the rearranged list, which we denote by $\mathcal{N}^\downarrow_{\text{new}}$. Figure 1 illustrates for an example with $N = 18$ objects and $K = 6$ antoclusters how the rearranged list $\mathcal{N}^\downarrow_{\text{new}}$ is constructed.

If N is not divisible by K , then we let $Q = \lfloor N/K \rfloor$ and $\bar{Q} = \lceil N/K \rceil$ denote the minimum and maximum size of an antocluster, respectively. The number of antoclusters with Q objects is $\bar{Q}K - N$ and the number of antoclusters

Algorithm 1 Assignment-based Anticlustering (ABA)

```

function ABA( $\mathcal{X} = \{\mathbf{x}_1, \dots, \mathbf{x}_N\}$ ,  $K$ )
    labels  $\leftarrow$  empty vector of size  $N$ 
    distances  $\leftarrow$  empty vector of size  $N$ 
     $\boldsymbol{\mu} \leftarrow \frac{1}{N} \sum_{i \in \mathcal{N}} \mathbf{x}_i$ 
    for  $i = 1$  to  $N$  do
        distances[ $i$ ]  $\leftarrow d(\mathbf{x}_i, \boldsymbol{\mu})$ 
    end for
     $\mathcal{N}^\downarrow \leftarrow \text{argsort}(\text{distances})$   $\triangleright$  Sort objects in descending order and store their indices in  $\mathcal{N}^\downarrow$ 
     $\mathcal{B}_1, \mathcal{B}_2, \dots, \mathcal{B}_B \leftarrow \text{split}(\mathcal{N}^\downarrow)$   $\triangleright$  Split  $\mathcal{N}^\downarrow$  into  $B = \lceil N/K \rceil$  batches
    labels[ $\mathcal{B}_1$ ]  $\leftarrow [1 \dots K]$   $\triangleright$  Assign one object from  $\mathcal{B}_1$  to each anticluster
    for  $k = 1$  to  $K$  do
         $i \leftarrow \mathcal{B}_1[k]$ 
         $\boldsymbol{\mu}_k \leftarrow \mathbf{x}_i$   $\triangleright$  Initialize the centroids of the  $K$  anticlusters
    end for
    for  $i = 2$  to  $B$  do
        costmatrix  $\leftarrow$  empty matrix of size  $|\mathcal{B}_i| \times K$   $\triangleright$  Initialize cost matrix
        for  $j = 1$  to  $|\mathcal{B}_i|$  do
            for  $k = 1$  to  $K$  do
                costmatrix[ $j$ ][ $k$ ]  $\leftarrow d(\mathbf{x}_{\mathcal{B}_i[j]}, \boldsymbol{\mu}_k)$   $\triangleright$  Compute squared Euclidean distances
            end for
        end for
        new_labels  $\leftarrow \text{SOLVE\_ASSIGNMENT\_PROBLEM}(\text{costmatrix})$ 
        for  $j = 1$  to  $|\mathcal{B}_i|$  do
             $k \leftarrow \text{new\_labels}[j]$ 
             $i' \leftarrow \mathcal{B}_i[j]$ 
             $\boldsymbol{\mu}_k \leftarrow \text{UPDATE\_CENTROID}(i, \boldsymbol{\mu}_k, \mathbf{x}_{i'})$ 
        end for
        labels[ $\mathcal{B}_i$ ]  $\leftarrow$  new_labels
    end for
    return labels
end function

function SOLVE_ASSIGNMENT_PROBLEM(costmatrix)
    assignment  $\leftarrow \text{LAPJV}(\text{costmatrix})$   $\triangleright$  LAPJV is a variant of the Jonker-Volgenant algorithm
    new_labels  $\leftarrow$  empty vector
    for each (row, col) in assignment do
        new_labels[row]  $\leftarrow$  col
    end for
    return new_labels
end function

function UPDATE_CENTROID(counter,  $\boldsymbol{\mu}_k$ ,  $\mathbf{x}_i$ )
    return  $\boldsymbol{\mu}_k + \frac{1}{\text{counter}}(\mathbf{x}_i - \boldsymbol{\mu}_k)$ 
end function

```

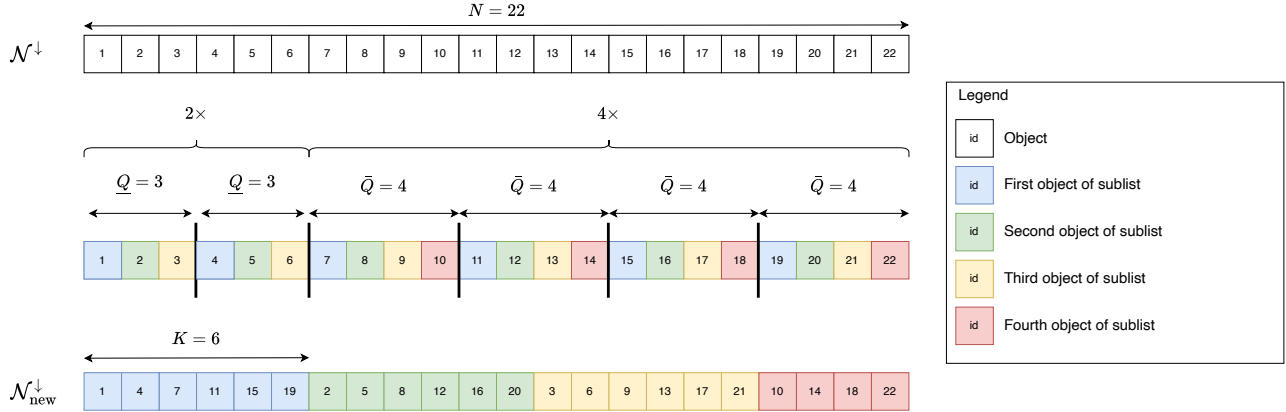


Figure 2: Illustration of how to rearrange the sorted list \mathcal{N}^\downarrow when N is not divisible by K based on an example with $N = 22$ objects and $K = 6$ antyclusters

with \bar{Q} objects is $N - QK$. We create the sublists such that the first $\bar{Q}K - N$ sublists have length Q and the remaining $N - QK$ sublists have length \bar{Q} . The rearranged list is created by repeatedly taking the first/next object from each sublist in order until Q objects have been taken from each sublist. The remaining $N - QK$ objects are then placed at the end of the rearranged list. The reason why we first have the shorter sublists is that the remaining $N - QK$ objects, which will form the last batch \mathcal{B}_B , are close to the global centroid and, therefore, less likely to significantly shift the antycluster centroids. The algorithm then continues with the rearranged list, which we denote by $\mathcal{N}_{\text{new}}^\downarrow$. Figure 2 illustrates for an example with $N = 22$ objects and $K = 6$ antyclusters how the rearranged list $\mathcal{N}_{\text{new}}^\downarrow$ is constructed.

As we demonstrated in Baumann et al. [2026], the ABA algorithm for small antyclusters is effective at producing high-quality solutions to the Euclidean maximum weight non-bipartite matching problem. In this special case of Euclidean antyclustering, each antycluster consists of exactly two objects. In the computational study of Baumann et al. [2026], we found that the ABA algorithm generates near-optimal matchings, often within less than one percent of the optimum. Moreover, ABA was often several orders of magnitude faster than exact approaches and other heuristics from the literature.

4.3 The ABA Algorithm With Categories

We also propose a variant of the ABA algorithm for the antyclustering problem with categories (see Section 2). The base version of the ABA algorithm requires two modifications to account for the additional constraint that all objects of the same category need to be evenly distributed across antyclusters.

The first modification rearranges the objects in the sorted list \mathcal{N}^\downarrow as follows. The list is divided into G sublists \mathcal{N}_g^\downarrow ($g \in G$), where each \mathcal{N}_g^\downarrow contains all objects belonging to category g , preserving their original order. Each \mathcal{N}_g^\downarrow is then partitioned into consecutive blocks of size K . If the number of objects in \mathcal{N}_g^\downarrow is not a multiple of K , the final block contains fewer than K objects. The rearranged list is obtained by sequentially concatenating all full (K -sized) blocks from the G lists in an alternating fashion, always selecting the next available block according to the sorting. The remaining (incomplete) blocks are appended at the end in the same alternating order. Figure 3 illustrates for an example with $N = 22$ objects and $K = 3$ antyclusters how to construct the rearranged list $\mathcal{N}_{\text{new}}^\downarrow$.

When splitting the rearranged list $\mathcal{N}_{\text{new}}^\downarrow$ into batches \mathcal{B}_1 to \mathcal{B}_B , the last batches may contain objects that belong to different categories. Because of this, we need to keep track of the number of objects of category $g \in G$ assigned to each antycluster $k \in K$ during the iterations. When an assignment of an object i to a antycluster k would violate the corresponding upper bound of $\lceil \frac{|\mathcal{N}_g|}{K} \rceil$, it is necessary to set the entry in the cost matrix that corresponds to the distance $d(\mathbf{x}_i, \mu_k)$ to a sufficiently large negative value (e.g., the negative maximum distance) prior to solving the assignment problem to ensure that the upper bound is never exceeded.

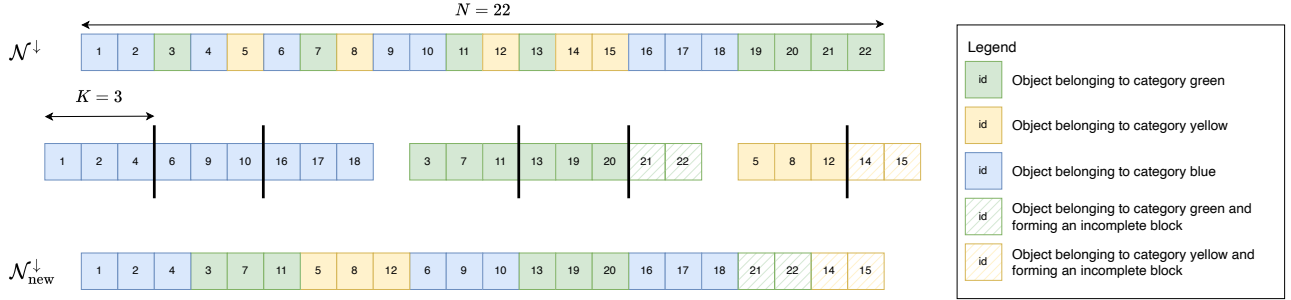


Figure 3: Illustration of how to rearrange the sorted list N^{\downarrow} to evenly distribute the categories of a categorical feature across antoclusters based on an example with $N = 22$ objects and $K = 3$ antoclusters.

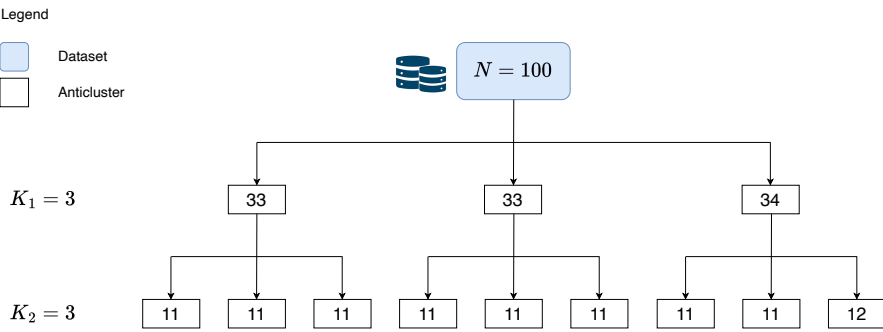


Figure 4: Illustration of the hierarchical decomposition strategy for a dataset with $N = 100$ objects and $K = 9$ antoclusters.

4.4 Computational Speed-Up with Hierarchical Decomposition

The size of the assignment problems solved during the execution of the ABA algorithm depends on K . For instances with large values of K , solving the assignment problems can become computationally prohibitive. For these instances, we propose a hierarchical decomposition strategy that achieves substantial reductions in running time while maintaining high solution quality. The idea is to construct the antoclusters in a hierarchical manner, i.e., first create K_1 antoclusters and then subdivide each of the K_1 antoclusters again into K_2 antoclusters. This will yield $K_1 \times K_2$ antoclusters. The number of levels L and the values K_1, K_2, \dots, K_L can be specified by the user. As stated in Lemma 1, a balanced decomposition in which the values of K_ℓ are as similar as possible, will deliver the lowest complexity for L levels. We also observe experimentally, in Figure 7, that such a choice does not noticeably diminish the quality of the solution. Note that the subproblems that result from the decomposition can be solved in parallel, leading to further improvements in the computational speed of the algorithm on multi-core machines. Figure 4 illustrates the hierarchical decomposition strategy based on an example with $N = 100$ objects and $K = 9$ antoclusters.

It can be shown that the hierarchical decomposition strategy proposed above still guarantees that the size of the final antoclusters lie within the prescribed bounds $\lfloor N/K \rfloor$ and $\lceil N/K \rceil$.

Proposition 1. *Applying hierarchical decomposition in L levels to an antoclustering problem on N objects and K antoclusters where at level ℓ each set of $N_\ell = \frac{N}{\prod_{i=1}^{\ell-1} K_i}$ objects is divided into K_ℓ parts whose sizes differ by at most one, then the final antoclusters, after L levels of recursion, also have sizes that differ by at most one, that is either $\lfloor N/K \rfloor$ or $\lceil N/K \rceil$.*

Proposition 1 follows from the fact that each balanced split preserves the correct number of “large” and “small” parts. At every recursive step, each set of $N_\ell = \frac{N}{\prod_{i=1}^{\ell-1} K_i}$ objects is divided into K_ℓ subsets of sizes $\lfloor N_\ell/K_\ell \rfloor$ and $\lceil N_\ell/K_\ell \rceil$, with exactly $N_\ell \bmod K_\ell$ subsets receiving one extra object. When these subsets are further partitioned, their extra objects propagate downward without creating additional imbalance, because every node is split in the same balanced manner. Consequently, after L levels the total of $N \bmod K$ extra objects is distributed across the

K final leaves, while all remaining leaves receive the baseline size. Thus, the final antoclusters have sizes $\lfloor N/K \rfloor$ or $\lceil N/K \rceil$, exactly as in a single direct balanced partition.

4.5 Runtime Complexity of the ABA Algorithm and the hierarchical decomposition

The time complexity of the base version of the ABA algorithm constitutes of the complexity of the steps:

- Computing the global centroid of the objects and their distances to the global centroid takes $O(ND)$ operations.
- Sorting the objects by decreasing distances to the global centroid takes $O(N \log N)$ time.
- Solving $\lceil N/K \rceil - 1$ assignment problems using the *LAPJV* algorithm, each requiring $O(K^3)$ operations, takes a total of $O(\frac{N}{K} K^3) = O(NK^2)$ time.

Hence, the overall time complexity of the ABA algorithm is $O(ND) + O(N \log N) + O(NK^2)$ or $O(N(D + \log N + K^2))$.

Since the calls to *LAPJV* dominate the running time, the running time is $O(NK^2)$. The time complexity is the same for the ABA algorithm for small antoclusters and the ABA algorithm with categories as the modifications with respect to the base version do not change the overall time complexity.

We next discuss the complexity of the hierarchical decomposition. To illustrate the total complexity expression consider the example of 3-level hierarchical decomposition with the choice of parameters K_1, K_2, K_3 . The complexity of ABA at each level is as follows:

- **Level 1.** ABA is applied once to the full instance with parameter K_1 , with complexity, $T_1 = O(NK_1^2)$, producing K_1 subproblems.
- **Level 2.** Each of the K_1 subproblems here contains approximately N/K_1 objects and is solved with parameter K_2 , partitioning each one of the K_1 subproblems to K_2 subproblems, for a total of $K_1 K_2$ subproblems. The total cost at this level is then $T_2 = K_1 \cdot O\left(\frac{N}{K_1} K_2^2\right) = O(NK_2^2)$.
- **Level 3.** Each of the $K_1 K_2$ resulting subproblems contains approximately $N/(K_1 K_2)$ objects and is solved with parameter K_3 . The total cost at this level is, $T_3 = K_1 K_2 \cdot O\left(\frac{N}{K_1 K_2} K_3^2\right) = O(NK_3^2)$.

Summing over all three levels yields $T_{\text{total}} = O(N(K_1^2 + K_2^2 + K_3^2))$.

Extrapolating from this 3-level example, the complexity of the hierarchical decomposition with L levels and parameters K_1, \dots, K_L is $T_\ell = O(NK_\ell^2)$ for level $\ell = 1, \dots, L$. The total complexity is then $\sum_{\ell=1}^L T_\ell = O\left(N \sum_{\ell=1}^L K_\ell^2\right)$.

The lemma below states that the selection of equal parameter values for K_ℓ minimizes the total complexity expression.

Lemma 1. *The optimal solution to $\{\min \sum_{\ell=1}^L K_\ell^2 \mid \prod_{\ell=1}^L K_\ell = K, K_\ell \geq 0\}$ is attained for $K_1 = \dots = K_L = K^{1/L}$.*

(The proof is straightforward and therefore omitted.) With this optimal choice, the total complexity of the hierarchical decomposition is $O(N L K^{2/L})$.

5 Experimental Analysis

In this section, we compare the performance of ABA with state-of-the-art algorithms in three experiments. First, we evaluate ABA against the algorithm of Papenberg and Klau [2021] for large-scale antoclustering in Euclidean space. Second, we assess the performance of ABA on antoclustering problem instances with categorical constraints, using the algorithms of Papenberg and Klau [2021] and Croella et al. [2025] as benchmarks. Third, we compare ABA to METIS (see Karypis and Kumar 1998), the leading algorithm for the balanced k -cut problem. The section is organized as follows. Section 5.1 introduces the datasets, Section 5.2 presents the benchmark algorithms, and Sections 5.3–5.5 report the experimental results.

Dataset	Objects (N)	Features (D)	Type	Source	Anticlustering paper
Abalone	4,177	10	Tabular	UCI ML Repository	Croella et al. [2025]
Travel	5,454	24	Tabular	UCI ML Repository	This paper
Facebook	7,050	13	Tabular	UCI ML Repository	Croella et al. [2025]
Frogs	7,195	22	Tabular	UCI ML Repository	Croella et al. [2025]
Electric	10,000	12	Tabular	UCI ML Repository	Croella et al. [2025]
Npi	10,440	40	Tabular	Online personality tests	Papenberg and Klau [2021]
Pulsar	17,898	8	Tabular	UCI ML Repository	Croella et al. [2025]
Creditcard	30,000	24	Tabular	UCI ML Repository	This paper
Adult	32,561	110	Tabular	UCI ML Repository	This paper
Plants	34,781	70	Tabular	UCI ML Repository	This paper
Bank	45,211	53	Tabular	UCI ML Repository	This paper
Cifar10	50,000	3,072	Image	UCI ML Repository	This paper
Mnist	60,000	784	Image	Kaggle	This paper
Survival	110,204	4	Tabular	UCI ML Repository	This paper
Diabetes	253,680	22	Tabular	UCI ML Repository	This paper
Music	515,345	91	Tabular	Kaggle	This paper
Covtype	581,012	55	Tabular	UCI ML Repository	This paper
Imagenet8	1,281,167	192	Image	ImageNet Image Database	This paper
Imagenet32	1,281,167	3,072	Image	ImageNet Image Database	This paper
Census	2,458,285	68	Tabular	UCI ML Repository	This paper
Finance	6,362,620	12	Tabular	Kaggle	This paper

Table 2: Overview of datasets

5.1 Datasets

We use a diverse set of datasets varying in the number of objects (N), the number of features (D), and the data type (tabular or image). Table 2 lists each dataset along with its source and the anticlustering paper where it has been used. Besides datasets from prior anticlustering research, we include additional datasets commonly used in machine learning. For datasets with categorical features, we encoded the categorical features as a set of binary features using a one-hot encoding scheme, creating one binary feature for each category. For datasets that included nonbinary features, we standardized all features by subtracting the mean and dividing by the standard deviation. Additional preprocessing was performed for specific datasets as described below. For the `Travel` dataset, we drop the `User` feature and remove objects with missing values. For the `Npi` dataset, we preprocessed the data in the same way as in Papenberg and Klau [2021], i.e., we removed objects with missing values and kept only the binary features representing the answers of the participants. For the `Creditcard` dataset, we leave out the `ID` feature. For the `Census` dataset, we drop the `caseid` feature. For the `Plants` dataset, we converted the original data into a binary matrix, with rows representing plants and columns representing states. An entry of one indicates that the plant occurs in the corresponding state. In the image datasets `Cifar10`, `Mnist`, `Imagenet8`, and `Imagenet32`, the features represent pixel intensities with values ranging from 0 to 255. As is commonly done with image data, we scaled the features by dividing them by 255 instead of standardizing them, bringing all values into the range [0,1]. Note that the `Imagenet8` and `Imagenet32` datasets are downsampled versions of the original ImageNet dataset, with image resolutions of 8×8 and 32×32 pixels, respectively. For the `Finance` dataset, we eliminated the features `step`, `nameOrig`, and `nameDest`.

5.2 Benchmark Algorithms

The benchmark algorithms used in the three experiments include the `fast-anticlustering` algorithm from the R package of Papenberg and Klau [2021], the integer linear programming model of Croella et al. [2025], the balanced k -cut algorithm from the METIS software package (see Karypis and Kumar 1998) and a random partitioning procedure. The R package `anticlust` of Papenberg and Klau [2021] includes several exact algorithms that are based on integer programming and an exchange-based heuristic. The exact algorithms are only able to solve small problem instances with up to 70 objects in acceptable running time. The exchange-based heuristic starts by randomly partitioning the objects into K equally-sized anticlusters. Then, for each object, it evaluates all possible swaps with objects in other anticlusters and performs the swap that yields the greatest improvement in the objective. By default, the algorithm stops after every object has been considered once. However, the user can choose that it does not terminate after the first loop over all objects and instead continues the swapping until a local maximum has been reached. With the default setting of stopping after the first loop, the heuristic is able to find solutions for problem instances with several hundred objects in acceptable running time. For datasets with thousands of objects, the R package `anticlust` additionally provides an exchange-based heuristic called `fast-anticlustering` that is

Abbr.	Name	Paper	Code	Link
ABA	Assignment-based antclustering	This paper	C	GitHub
P-N5	Fast-anticlustering with 5 nearest-neighbor exchange partners	Papenberg and Klau [2021]	C	GitHub
P-R5	Fast-anticlustering with 5 random exchange partners	Papenberg and Klau [2021]	C	GitHub
P-R50	Fast-anticlustering with 50 random exchange partners	Papenberg and Klau [2021]	C	GitHub
P-R500	Fast-anticlustering with 500 random exchange partners	Papenberg and Klau [2021]	C	GitHub
MILP	MILP model of AVOC algorithm	Croella et al. [2025]	C	GitHub
METIS	Balanced K -cut algorithm from METIS	Karypis and Kumar [1998]	C	GitHub
Rand	Random partitioning	This paper	C	GitHub

Table 3: Overview of all algorithms used in the experimental analysis

specifically designed for large-scale instances. It works in the same way as the standard exchange-based heuristic, but considers only a user-defined number of exchange partners for each object. The default behaviour is to generate exchange partners by using a nearest neighbor search. Using more exchange partners tends to improve the quality of the solution, but increases running time. To avoid running the nearest neighbor search, the exchange partners can be chosen randomly. In our experiments, we only compare to the **fast-anticlustering** algorithm because it is the only one that scales to large-sized instances with more than 10,000 objects. In Papenberg and Klau [2021], the **fast-anticlustering** algorithm is applied with 5 exchange partners determined by nearest neighbour search. We run it with the same settings and in addition with 5, 50, and 500 randomly generated exchange partners. To the best of our knowledge, the **fast-anticlustering** algorithm is the leading algorithm for large-scale antclustering. We applied the balanced k -cut algorithm from the METIS software package with its default control parameter values. It requires an input file that specifies all neighbors for each node of the graph together with the corresponding edge weights as integers. The tests of METIS versus ABA are described in Section 5.5.

Table 3 lists each algorithm together with its abbreviation, full name, source publication, programming language, and a link to its source code.

5.3 Comparison to Leading Algorithms on Standard Anticlustering Problems

In this experiment, we compare the ABA algorithm with the **fast-anticlustering** algorithm of Papenberg and Klau [2021] on 16 datasets containing up to 6.3 million objects and 3,072 features. The **fast-anticlustering** algorithm was run with the same configuration as in Papenberg and Klau [2021], using 5 exchange partners determined via nearest-neighbor search (denoted P-N5). Additionally, we applied the algorithm with 5, 50, and 500 randomly chosen exchange partners (P-R5, P-R50, P-R500). As a baseline, we used random partitioning (Rand). The ABA algorithm is deterministic, whereas the other algorithms are stochastic and require a random seed. We ran each benchmark algorithm three times per problem instance and report the average metrics below. We stopped a run if a time limit of two hours has been reached. Table 4 presents the results for $K = 5$. The first three columns list the name of the dataset, the number of objects (N), and the number of features (D). Column 4 reports the objective function values for the solutions obtained by the ABA algorithm (ofv ABA), computed here as the sum of squared Euclidean distances between the objects and their corresponding anticluster centroid. Columns 5–8 show the percentage deviation of the objective function values obtained by the benchmark algorithms from that of ABA. A negative deviation indicates that the ABA algorithm outperformed the respective algorithm. A dash (—) means that the respective algorithm did not return a solution within the prescribed time limit of two hours in any of the three runs. Column 10 gives the running time of the ABA algorithm in seconds, while columns 11–14 report the percentage deviations of the running time of the **fast-anticlustering** algorithms from that of ABA. A positive deviation indicates that the respective algorithm is slower than the ABA algorithm. To compute the average, the bottom row of the table, we exclude the dash-entries and take the average only across the entries where the respective algorithm computed a solution.

From Table 4, we observe that ABA and the **fast-anticlustering** algorithms (P-N5, P-R5, P-R50, P-R500) achieve comparable solution quality, whereas Rand performs slightly worse. However, while ABA computes the solution for each dataset in under a second or just a few seconds, P-N5, P-R5, P-R50, and P-R500 are substantially slower, with average running times up to three orders of magnitude longer than those of ABA. We generated additional tables for $K = \{2, 50, 500, 1,000, 2,000, 5,000\}$ that have the same structure as Table 4. These tables are available on [GitHub](#)². Note that for large instances, we applied ABA with hierarchical decomposition. Table 5 specifies the settings we used for the hierarchical decomposition as a function of the number of objects (N) and the number of anticlusters (K). For larger values of K , the ABA algorithm not only outperforms the

²<https://github.com/phil85/aba-results>

Dataset	N	D	ofv ABA	Deviation from ofv ABA [%]					cpu ABA [s]	Deviation from cpu ABA [%]			
				P-N5	P-R5	P-R50	P-R500	Rand		P-N5	P-R5	P-R50	P-R500
Travel	5,454	24	130,871.89	0.0001	0.0000	0.0001	0.0001	-0.0192	0.002	45,104.8	34,479.4	44,869.6	129,328.6
Npi	10,440	40	87,153.59	0.0000	0.0000	0.0000	0.0000	-0.0320	0.004	255,033.1	33,576.3	47,813.8	156,944.4
Creditcard	30,000	24	719,975.99	0.0000	0.0000	0.0000	0.0000	-0.0160	0.010	76,110.7	36,331.0	47,208.7	119,590.6
Adult	32,561	110	3,581,588.43	-0.0048	0.0000	0.0000	0.0000	-0.0121	0.025	48,457.0	18,036.4	32,013.6	143,843.5
Plants	34,781	70	258,111.51	0.0000	0.0000	0.0000	0.0000	-0.0083	0.019	94,101.5	25,195.4	37,595.0	125,792.1
Bank	45,211	53	2,396,129.86	-0.0017	0.0000	0.0000	0.0000	-0.0051	0.024	65,465.5	26,216.3	39,325.8	126,328.3
Cifar10	50,000	3,072	9,520,045.51	0.0000	-0.0001	0.0000	0.0000	-0.0105	0.682	610,874.4	10,035.1	79,509.9	761,007.1
Mnist	60,000	784	3,163,501.01	0.0000	0.0000	0.0000	0.0000	-0.0062	0.223	1,362,505.0	9,737.3	57,277.3	528,621.2
Survival	110,204	4	440,812.00	-0.0038	0.0000	0.0000	0.0000	-0.0026	0.024	60,549.7	58,127.1	72,821.1	123,547.4
Diabetes	253,680	22	5,580,938.00	-0.0003	0.0000	0.0000	0.0000	-0.0015	0.145	87,496.1	24,957.1	32,754.8	76,951.9
Music	515,345	91	46,896,303.99	—	0.0000	0.0000	0.0000	-0.0006	0.483	—	16,723.4	30,304.8	155,567.6
Covtype	581,012	55	31,955,602.87	-0.0005	0.0000	0.0000	0.0000	-0.0002	0.394	28,849.3	22,816.1	36,154.8	142,034.4
Imagenet8	1,281,167	192	13,327,181.18	—	0.0000	0.0000	0.0000	-0.0003	1.872	—	12,095.5	30,794.8	203,514.9
Imagenet32	1,281,167	3,072	265,674,709.96	—	—	—	—	-0.0003	17.733	—	—	—	—
Census	2,458,285	68	167,163,312.00	—	0.0000	0.0000	0.0000	-0.0002	2.342	—	16,299.1	28,130.4	128,512.1
Finance	6,362,620	12	76,351,427.75	0.0000	0.0000	0.0000	—	4.532	24,387.9	20,434.0	26,493.8	—	—
Average				-0.0009	0.0000	0.0000	0.0000	-0.0072		229,911.3	24,337.3	42,871.2	208,684.6

ABA is the contribution in this paper

Table 4: Comparing solution quality and running times for $K = 5$ of ABA, P-N5, P-R5, P-R50, P-R500, and random. Reported are the objective function values (ofv) for the ABA algorithm and the percentage deviations from these values for the other algorithms (positive deviation means improving on ABA). Also reported are the running times of the ABA algorithm in seconds (cpu) and the percentage deviations from these values for the other algorithms (negative deviation means improving on ABA). A dash indicates that the algorithm did not return a solution within the prescribed time limit of two hours in any of the three runs.

K							
2	5	50	500	1,000	2,000	5,000	
$N \leq 50,000$	—	—	—	—	(2×500)	(4×500)	(10×500)
$N > 50,000$	—	—	—	(4×125)	(8×125)	(16×125)	(40×125)

Table 5: The settings used for hierarchical decomposition as a function of the number of objects (N) and the number of anticlusters (K). A dash (—) indicates that hierarchical decomposition was not applied. The expression $(K_1 \times K_2)$ denotes a decomposition with two levels and $K = K_1 \times K_2$.

fast-anticlustering algorithms in terms of speed, but also in terms of solution quality. The outperformance in terms of solution quality increases with larger values of K .

A further analysis showed that the ABA algorithm produces anticlusters which are very similar to each other in terms of diversity. We measured the diversity of an anticluster as the sum of squared distances between its assigned objects and its centroid. The bechmark approaches P-N5, P-R5, P-R50, P-R500, and Rand tend to produce anticlusters that are far less balanced in terms of diversity. To quantify the similarity of anticlusters within a solution, we compute, for each of the K anticlusters, the diversity, i.e., the sum of squared distances between the assigned objects and the corresponding centroid. Based on these K values, we then calculate two statistics, namely the standard deviation (sd) and the range (range) obtained with ABA, respectively. The columns 5–9 provide for each benchmark algorithm the percentage deviations from the standard deviations of ABA. Analogously, columns 11–15 provide for each benchmark algorithm the percentage deviations from the range values of ABA. Positive deviations indicate that the corresponding benchmark algorithm produced a solution with a higher standard deviation or larger range. From Table 6, we observe that the ABA algorithm consistently produces anticlusters with more balanced diversity. The same conclusion can be drawn for $K = \{2, 50, 500, 1,000, 2,000, 5,000\}$ as can be seen in the corresponding tables on [GitHub](#)².

We observed the largest differences in terms of balanced diversity between the ABA algorithm and the benchmark algorithms for the image datasets Mnist, Cifar10, Imagenet8, and Imagenet32 when K is large. Figure 5 shows the distributions of the anticluster diversity values for the solutions obtained with ABA and P-R5 with $K = 2,000$. For the dataset Imagenet32, the P-R5 algorithm found no solution within the time limit of two hours. We therefore compare ABA and Rand for this dataset. The diversity distributions of ABA exhibit not only higher means, but also smaller spreads than the diversity distributions of P-R5 and Rand.

To further illustrate the balanced diversity of anticlusters produced by ABA, we looked at the distribution of distances within anticlusters. Figure 6 visualizes for the Travel dataset with $K = 50$ the distribution of

$K = 5$

Dataset	N	D	Deviation from sd ABA [%]					range ABA [s]	Deviation from range ABA [%]						
			sd ABA	P-N5	P-R5	P-R50	P-R500		P-N5	P-R5	P-R50	P-R500	Rand		
Travel	5,454	24	4.8	7,667.8	3,608.7	3,631.3	4,152.6	3,082.9	13.3	7,821.7	3,518.5	3,689.9	4,207.4	3,332.3	
Npi	10,440	40	0.3	245.0	440.8	280.8	466.0	27,579.4	0.9	226.3	406.2	282.4	354.1	26,261.8	
Creditcard	30,000	24	2,475.4	114.7	115.2	103.9	122.7	208.2	6,985.7	102.2	114.5	88.0	125.3	202.9	
Adult	32,561	110	11,616.3	31.2	2.6	24.5	6.4	69.6	29,830.0	35.7	14.3	33.0	13.6	84.5	
Plants	34,781	70	0.9	997.3	635.1	823.1	947.5	66,157.8	2.9	932.1	597.4	727.5	919.6	62,448.5	
Bank	45,211	53	5,303.9	11.4	7.9	-2.4	1.7	-2.7	13,524.9	17.8	14.8	1.4	5.6	4.7	
Cifar10	50,000	3,072	38.4	19,311.3	21,843.0	27,201.3	20,001.0	23,785.2	98.9	21,663.2	23,558.9	29,167.5	20,656.8	27,983.1	
Mnist	60,000	784	3.9	5,659.0	3,781.6	3,837.8	4,381.2	31,747.0	10.6	5,838.0	3,671.2	3,822.8	4,250.1	31,659.9	
Survival	110,204	4	3.6	19,239.1	5,936.4	8,222.4	8,351.9	12,514.1	9.5	18,843.9	6,215.4	8,744.6	9,263.3	13,148.7	
Diabetes	253,680	22	6.5	40,109.3	13,297.6	12,622.8	10,853.3	43,579.7	15.6	45,253.3	15,983.7	15,023.4	12,706.3	44,789.9	
Music	515,345	91	5,872.7	—	322.2	408.4	452.0	794.0	16,478.4	—	314.6	389.2	431.7	785.1	
Covtype	581,012	55	93,564.1	13.1	1.0	1.6	1.0	37.8	192,502.9	40.4	3.0	2.8	2.0	68.1	
Imagenet8	1,281,167	192	0.8	—	227,728.0	243,564.5	451,199.2	433,347.3	2.3	—	247,409.1	242,311.0	482,542.0	454,750.8	
Imagenet32	1,281,167	3,072	8.0	—	—	—	—	568,933.2	21.9	—	—	—	—	608,410.1	
Census	2,458,285	68	68.2	—	4,940.4	5,782.9	6,532.9	50,867.9	185.3	—	5,122.2	5,648.2	6,828.8	56,229.6	
Finance	6,362,620	12	151,605.7	289.7	34.0	18.8	—	341.9	382,057.0	338.4	47.4	28.8	—	394.8	
Average				7,807.4	18,846.3	20,434.8	36,247.8	78,940.2			8,426.1	20,466.1	20,664.0	38,736.2	83,159.7

ABA is the contribution in this paper

Table 6: Comparing the statistics of the solutions produced by ABA, P-N5, P-R5, P-R50, P-R500 and random. Reported are the standard deviations (sd) of the diversity values of the $K = 5$ antoclusters produced by the ABA algorithm and the percentage deviations from these values for the other algorithms (negative deviation means improving on ABA). Also reported are the ranges (range) of the diversity values of the $K = 5$ antoclusters (max diversity - min diversity) produced by the ABA algorithm and the percentage deviations from these values for the other algorithms (negative deviation means improving on ABA). A dash indicates that the algorithm did not return a solution within the prescribed time limit of two hours.

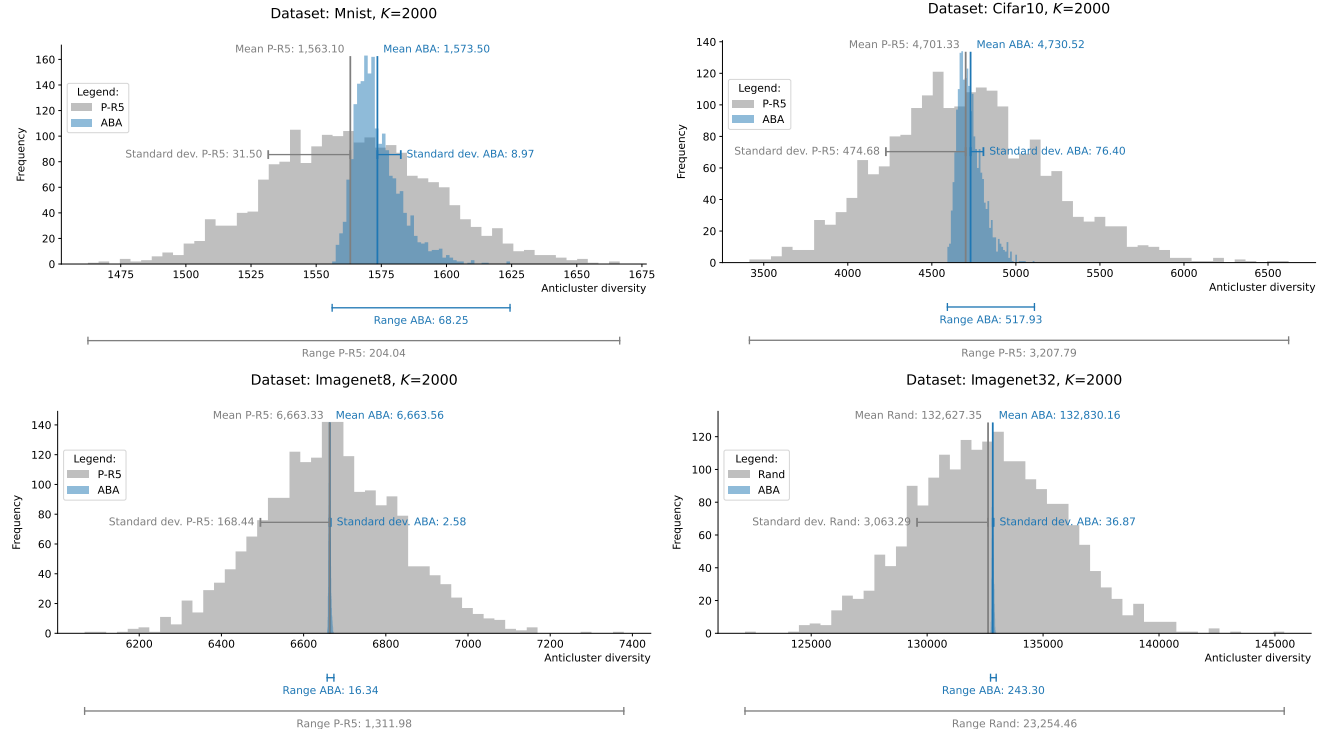


Figure 5: Comparison of distribution of anticluster diversity values between ABA and P-R5 for $K = 2,000$. For the dataset Imagenet32, the P-R5 algorithm found no solution within the time limit of two hours. We therefore compare ABA and Rand for this dataset.

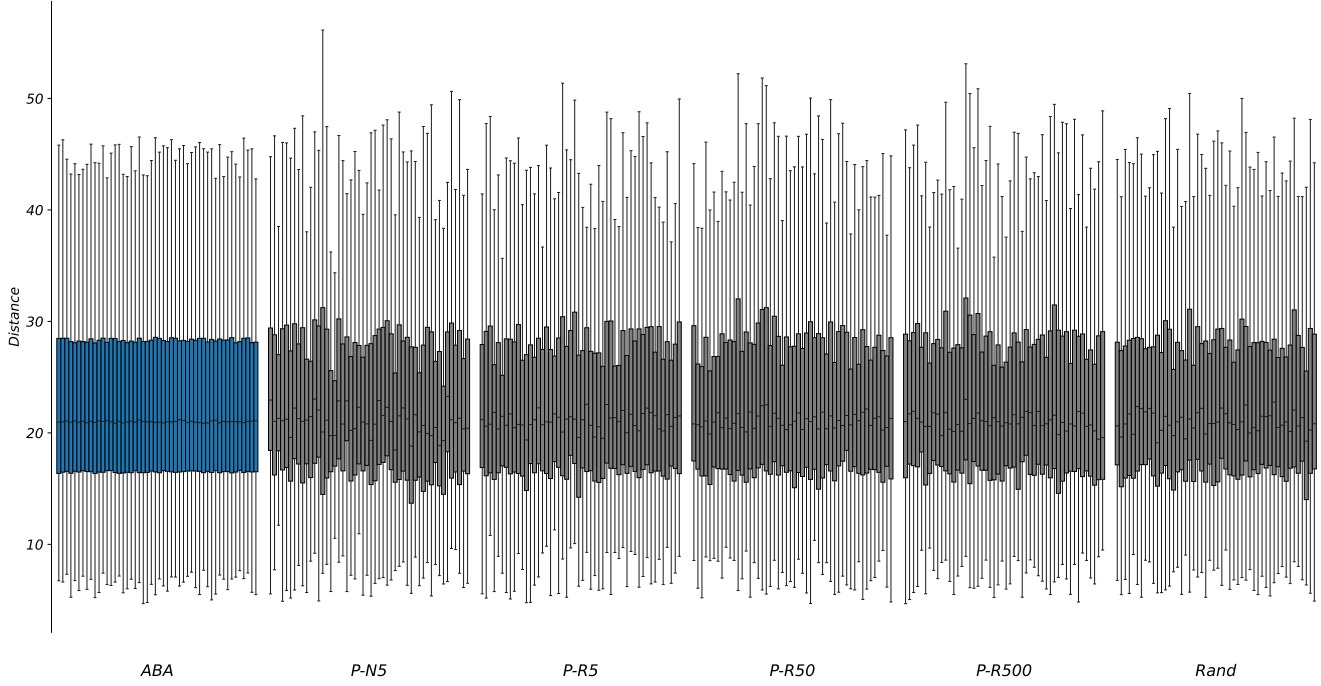


Figure 6: Comparison of distance distributions within antoclusters for the **Travel** dataset with $K = 50$. For each algorithm, 50 boxplots are shown. Each boxplot shows the distribution of distances between the objects and the center of an antocluster. The outliers have been removed for clarity.

distances within antoclusters for the solutions obtained by **ABA** and the benchmark algorithms. For each algorithm, 50 boxplots are shown, one for each antocluster. Each boxplot shows the distribution of distances between the objects and the centroid of the antocluster. The outliers have been removed for clarity. We can see that the **ABA** algorithm produces antoclusters with very similar distance distributions, whereas the benchmark algorithms yield antoclusters with highly varying distance distributions. The **ABA** algorithm produces antoclusters with similar distance distribution because it first sorts all objects by their distance to the global centroid and then splits them into batches of size K . This ensures that the objects in each batch have similar distances to the global centroid and since antocluster centroids tend to be close to the global centroid in final solutions, each antocluster gets one object from each distance range.

The hierarchical decomposition strategy presented in Section 4.4 allows the **ABA** algorithm to compute high-quality solutions for large values of K in short running time. To illustrate the effectiveness of this strategy, we applied different hierarchical settings on the **Imagenet32** dataset with $N = 1,281,167$ objects and $D = 3,072$ features for $K = 5,000$. Figure 7 compares the running times and normalized objective function values for different two-level hierarchical strategies to the base version of **ABA** that uses no hierarchical decomposition. With no hierarchical decomposition, the **ABA** algorithm requires more than 3,900 seconds to compute a solution. By applying hierarchical decomposition, the running time can be drastically reduced to 44.3 seconds with only a marginal deterioration in the objective function value (-0.013%). As observed experimentally in Figure 7, the quality of the solution is not noticeably affected by the selected decomposition of K . However, the running times are dramatically improved by choosing a decomposition where the values of K_i are as balanced as possible.

With hierarchical decomposition, the **ABA** algorithm can handle even much larger values of K . To demonstrate this capability, we applied **ABA** with $K = \{10,000, 20,000, 40,000, 80,000, 160,000, 320,000, 640,000\}$ to the **Imagenet32** dataset which has $N = 1,281,167$ objects. Table 8 lists the running times and the objective function values for **ABA**. For these instances, we applied the **ABA** algorithm with the hierarchical decomposition settings provided in Table 7. The only benchmark approach that was able to produce solutions within a time limit of two hours was random partitioning (Rand). We can see from Table 8 that **ABA** clearly outperforms Rand in terms of solution quality for all considered values of K . The absolute percentage deviation of the objective function values of Rand from those of **ABA** increases with larger values of K . The **ABA** algorithm obtains solutions that are over 30% better than those of Rand for $K = 640,000$.

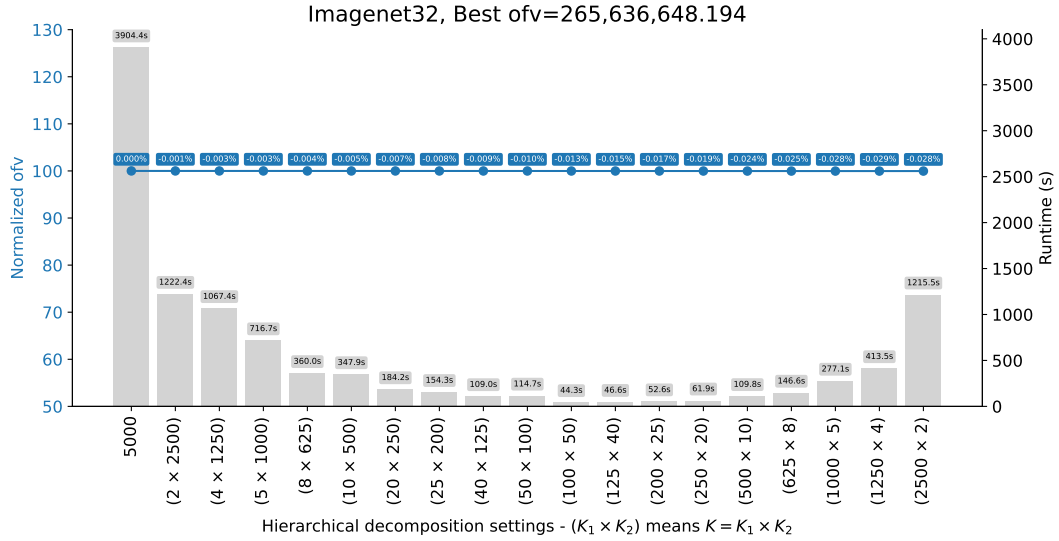


Figure 7: Comparison of objective function values (ofv) and running times (cpu) for different hierarchical decomposition strategies. Each setting produces $K = 5,000$ antoclusters for the Imagenet32 dataset. The blue line shows the normalized objective function values for the different settings with labels indicating the percentage deviation from the best setting (see left axis). The gray bars represent the running time in seconds for the different settings (see right axis).

	K						
	10,000	20,000	40,000	80,000	160,000	320,000	640,000
Imagenet32	(50 x 200)	(100 x 200)	(200 x 200)	(2 x 200 x 200)	(4 x 200 x 200)	(8 x 200 x 200)	(16 x 200 x 200)

Table 7: The hierarchical decomposition settings used for the Imagenet32 dataset as a function of the number of antoclusters (K). The expression $(K_1 \times K_2 \times K_3)$ denotes a decomposition with three levels and $K = K_1 \times K_2 \times K_3$.

Dataset: Imagenet32 ($N=1,281,167$, $D=3,072$)						
K	Min size	Max size	cpu ABA [s]	ofv ABA	ofv Rand	Deviation [%]
10,000	128	129	87.9	265,506,874.2	263,596,017.4	-0.7197
20,000	64	65	88.5	265,211,753.5	261,523,122.1	-1.3908
40,000	32	33	106.4	264,440,895.2	257,383,295.3	-2.6689
80,000	16	17	138.7	262,466,218.2	249,093,874.6	-5.0949
160,000	8	9	175.0	257,433,000.0	232,437,686.9	-9.7094
320,000	4	5	254.9	244,033,085.9	199,315,726.3	-18.3243
640,000	2	3	456.5	191,492,745.8	132,899,446.9	-30.5982

ABA is the contribution in this paper

Table 8: Comparing solution quality of ABA and Rand on the Imagenet32 dataset for large values of k . Reported are the objective function values (OFV) of both algorithms as well as the percentage deviation of the Rand values from the ABA values. Columns 2 and 3 state the minimum and maximum number of objects in an antocluster and column 5 reports the running time of ABA. The algorithms P-N5, P-R5, P-R50, and P-R500 were not able to find solutions for such large values of k .

5.4 Application of ABA to Anticlustering Problems with Categories

In some applications, it is desirable to distribute the values of a categorical feature evenly across anticlusters (see, e.g., Croella et al. 2025). In Section 4.3, we presented an extension of the ABA algorithm that ensures a balanced distribution of a categorical feature across anticlusters. In this section, we compare the performance of this extension with state-of-the-art benchmark algorithms from the literature. The benchmark algorithms for this comparison include the MILP model of the AVOC algorithm (see Croella et al. 2025) and the versions of the **fast-anticlustering** algorithm from Papenberg and Klau [2021] that can consider a categorical feature. Specifically, we consider the versions P-R5, P-R50, and P-R500, which use 5, 50, and 500 randomly generated exchange partners, respectively (see Table 3). The version P-N5, which selects the five nearest neighbors of an object as exchange partners, cannot account for a categorical feature because it cannot guarantee that the exchange partners belong to the same category as the object itself. For the version P-R5, P-R50, and P-R500, this requirement can be enforced with the function `generate_exchange_partners()`. To solve the MILP model of the AVOC algorithm, we used the Gurobi solver 12.0. We further include here as a baseline a version of random partitioning that accounts for a categorical feature (Rand). We use the same five real-world datasets as in Croella et al. [2025]. For each dataset, we generated the categorical feature by applying the k -means clustering algorithm. We set the number of anticlusters to the values reported in Croella et al. [2025], i.e., four anticlusters for the dataset **Frogs**, three for the datasets **Abalone**, **Facebook**, and **Electric**, and two for the dataset **Pulsar**. The labels returned by the k -means algorithm were used as the values for the categorical feature. For each of the five datasets, Croella et al. [2025] tested five different values for the number of anticlusters, which yields 25 instances in total. We applied the MILP model and the ABA algorithm once to each instance. The three variants of the **fast-anticlustering** algorithm and the random partitioning approach were each applied three times per instance, and average metrics were reported.

Table 9 provides the results. The first four columns list the name of the dataset, the number of objects (N), the number of features (D), and the number of anticlusters (K). Column 5 reports the objective function values of the solutions obtained by the ABA algorithm (ofv ABA), computed here as the sum of squared Euclidean distances between the objects and their corresponding anticluster centroid. Columns 6–10 show the percentage deviation of the objective function values obtained by the benchmark algorithms from that of ABA. A negative deviation indicates an outperformance of the ABA algorithm. Column 11 gives the running time of the ABA algorithm in seconds, while columns 12–15 report the percentage deviations of the running time of the MILP model and the **fast-anticlustering** algorithms from that of ABA. A positive deviation indicates that the respective algorithm is slower than the ABA algorithm. The bottom row of the table reports the respective average deviations.

Table 9 shows that ABA consistently outperforms the MILP model and Rand in both quality and speed. It matches the fast-clustering variants (P-R5, P-R50, P-R500) in solution quality but computes solutions up to three orders of magnitude faster.

As in the previous experiment, we calculated for each solution the diversity for each of the K anticlusters separately and then based on these K values calculated the standard deviation (sd) and the range (difference between maximum and the minimum). Table 10 reports both metrics for all 25 instances. Consistent with the earlier results, the ABA algorithm produces anticlusters with more balanced diversity than the other methods.

5.5 Application of ABA to Balanced Cut and Balanced k -Cut

The balanced cut problem consists of partitioning the nodes of a graph into two equally sized anticlusters such that the sum of edge weights between the anticlusters (the cut cost) is minimized. The balanced cut problem generalizes to the balanced k -cut problem, where the nodes are partitioned into K equal-sized anticlusters with the goal of minimizing the total edge weight between different anticlusters. In the case of tabular data, where the underlying graph is complete and the edge weights represent squared Euclidean distances between the corresponding objects (or data points), minimizing the cut cost corresponds to maximizing the within-anticluster sum of squared distances. Because of that equivalence, we can use the ABA algorithm for the balanced K -cut problem of tabular data. In this section, we compare the ABA algorithm to METIS, the state-of-the-art algorithm for solving balanced cut and balanced K -cut problems. While the ABA algorithm takes the dataset $\mathcal{X} = \{\mathbf{x}_1, \dots, \mathbf{x}_N\}$ and the number of anticlusters K as input, the METIS algorithm requires a graph representation in the form of an adjacency list with edge weights in addition to the number of anticlusters. Constructing such a representation for large datasets and running METIS on it is computationally and memory intensive. Consequently, for this comparison, we considered only datasets with fewer than 50,000 objects and for each object, we only list $p = 30$ randomly selected neighbors with the corresponding edge weights. In our experiments, using larger values for p or selecting the p neighbors according to the weight of the corresponding edges did not improve the quality of the solutions obtained with

Dataset	N	D	K	Deviation from ofv ABA [%]							Deviation from cpu ABA [%]						
				ofv ABA	AVOC-MILP	P-R5	P-R50	P-R500	Rand	cpu ABA [s]	AVOC-MILP	P-R5	P-R50	P-R500			
Abalone	4,177	10	4	41,759.99	-1.2553	0.0000	0.0000	0.0000	-0.0317	0.002	10,674.6	62,001.8	67,255.9	117,917.1			
			5	41,759.98	-1.1358	0.0000	0.0000	0.0000	-0.0403	0.002	12,923.5	62,052.6	67,745.3	120,525.0			
			6	41,759.98	-1.3272	0.0000	0.0000	0.0000	-0.0461	0.002	19,285.3	58,284.5	64,125.2	114,770.1			
			8	41,759.97	-1.7711	0.0000	0.0000	0.0000	-0.0838	0.002	42,450.9	49,810.9	54,246.0	97,610.5			
			10	41,759.94	-1.8276	0.0000	0.0000	0.0000	-0.1383	0.002	113,170.1	43,891.4	48,550.6	87,483.7			
Facebook	7,050	13	7	91,636.97	-5.3732	0.0000	0.0000	0.0000	-0.0564	0.003	21,057.7	162,745.9	170,773.2	210,257.3			
			8	91,636.83	-5.7497	0.0000	0.0000	0.0000	-0.0721	0.003	31,800.2	155,585.5	166,008.6	201,412.7			
			10	91,636.56	-5.9977	0.0000	0.0000	0.0000	-0.1047	0.003	62,758.4	135,299.4	142,275.9	176,330.6			
			13	91,636.56	-7.2956	-0.0001	0.0000	0.0000	-0.1355	0.004	230,917.9	109,088.5	115,277.2	142,208.9			
			18	91,635.42	-7.6534	-0.0004	0.0000	0.0000	-0.1819	0.005	694,918.4	86,441.2	91,161.3	113,085.2			
Frogs	7,195	22	8	158,267.92	-7.0749	0.0000	0.0000	0.0000	-0.0230	0.003	92,477.9	83,810.8	92,164.3	146,892.0			
			10	158,267.86	-10.6908	0.0000	0.0001	0.0001	-0.0290	0.004	190,892.7	64,936.5	71,885.6	115,655.0			
			13	158,267.77	-11.0695	-0.0001	0.0001	0.0001	-0.0380	0.005	565,602.4	57,763.8	63,695.7	104,303.4			
			15	158,267.73	-12.4326	-0.0002	0.0001	0.0001	-0.0512	0.005	1,032,629.8	50,736.5	56,089.3	92,309.0			
			16	158,267.67	-11.1633	-0.0002	0.0001	0.0001	-0.0490	0.005	1,488,430.2	48,157.9	53,626.8	87,766.3			
Electric	10,000	12	10	119,987.95	-0.0837	0.0000	0.0000	0.0000	-0.0807	0.004	71,594.5	95,408.6	105,213.4	139,266.3			
			15	119,987.90	-0.1197	0.0000	0.0000	0.0000	-0.1346	0.006	331,436.3	76,148.2	84,223.1	111,355.9			
			20	119,987.83	-0.1761	-0.0001	0.0000	0.0001	-0.1889	0.007	603,941.7	58,501.0	64,829.7	86,725.9			
			25	119,987.78	-0.2124	-0.0001	0.0000	0.0001	-0.2505	0.009	2,731,703.5	48,312.9	53,153.6	71,429.4			
			30	119,987.71	-0.2500	-0.0003	0.0000	0.0001	-0.2947	0.010	8,400,840.5	41,976.9	46,230.5	61,967.7			
Pulsar	17,898	8	18	143,176.00	-0.7841	0.0000	0.0000	0.0000	-0.0775	0.015	46,765.3	155,314.3	158,364.8	171,143.6			
			20	143,176.00	-0.7946	0.0000	0.0000	0.0000	-0.0951	0.016	61,015.3	143,480.4	147,193.5	159,381.6			
			25	143,176.00	-1.0012	0.0000	0.0000	0.0000	-0.1160	0.021	87,135.8	111,041.4	113,488.9	122,974.5			
			30	143,175.99	-1.0790	0.0000	0.0000	0.0000	-0.1452	0.025	154,599.0	93,264.9	95,536.1	103,859.7			
			35	143,175.99	-1.2821	-0.0001	0.0000	0.0000	-0.1600	0.030	232,183.3	78,080.6	79,395.5	86,167.5			
Average					-3.9040	-0.0001	0.0000	0.0000	-0.1050			693,248.2	85,285.5	90,900.4	121,712.0		

ABA is the contribution in this paper

Table 9: Comparing solution quality and running times of ABA, P-R5, P-R50, P-R500, and random for instances with a categorical feature. Reported are the objective function values (ofv) for the ABA algorithm and the percentage deviations from these values for the other algorithms (positive deviation means improving on ABA). Also reported are the running times of the ABA algorithm in seconds (cpu) and the percentage deviations from these values for the other algorithms (negative deviation means improving on ABA).

Dataset	N	D	K	Deviation from sd ABA [%]							Deviation from range ABA [%]						
				sd ABA	AVOC-MILP	P-R5	P-R50	P-R500	Rand	range ABA	AVOC-MILP	P-R5	P-R50	P-R500	Rand		
Abalone	4,177	10	4	204.4	116.9	28.6	11.8	70.6	33.6	501.8	126.9	38.3	14.6	87.7	28.0		
			5	190.6	94.5	23.5	33.8	42.4	54.2	498.4	85.5	32.6	38.2	52.6	64.9		
			6	177.8	118.5	54.5	52.2	59.2	31.1	496.6	132.4	76.9	66.4	75.6	31.6		
			8	165.9	64.9	38.2	46.1	51.0	32.5	526.6	73.3	45.8	59.2	67.9	38.9		
			10	148.9	90.1	14.7	35.3	53.9	35.5	512.2	98.1	25.4	40.7	73.5	48.2		
Facebook	7,050	13	7	470.9	749.5	151.1	124.6	100.9	174.4	1,320.1	710.2	147.7	122.1	122.8	215.0		
			8	463.7	660.5	216.9	129.4	167.3	161.8	1,299.2	757.7	289.3	158.6	194.9	228.7		
			10	376.2	740.7	230.5	238.3	188.4	254.2	1,069.7	897.3	302.8	298.0	236.1	309.2		
			13	450.6	497.8	88.8	103.3	116.3	160.1	1,527.9	493.4	102.3	101.4	126.1	197.1		
			18	427.0	455.4	94.1	99.6	82.9	118.0	1,458.0	442.6	112.8	103.9	97.6	147.4		
Frogs	7,195	22	8	44.1	9,162.3	591.6	799.6	760.4	1,008.0	152.3	7,162.4	524.9	730.2	665.6	942.6		
			10	58.4	5,152.0	352.4	405.2	370.5	552.0	213.0	4,679.1	289.1	352.5	325.6	459.0		
			13	52.6	4,206.2	375.0	422.8	379.7	515.4	211.4	3,163.6	334.3	371.4	334.5	392.1		
			15	53.1	3,863.6	330.3	291.3	297.3	502.7	186.8	3,601.9	317.8	292.3	345.8	470.9		
			16	54.0	3,666.5	308.9	306.1	319.1	510.5	212.0	2,933.6	275.4	319.5	270.5	416.5		
Electric	10,000	12	10	2.1	4,127.7	5,608.5	5,966.3	6,039.4	4,550.0	8.0	3,450.2	4,476.3	4,795.5	5,255.0	4,146.5		
			15	2.6	2,252.6	3,231.1	3,617.7	3,197.0	2,510.2	9.4	2,009.0	2,991.9	3,018.1	2,789.2	2,792.4		
			20	3.0	2,121.5	2,611.9	2,737.8	2,385.0	2,457.0	12.7	1,653.9	2,095.1	2,066.9	1,981.3	2,188.8		
			25	2.4	2,380.2	2,689.3	2,543.3	2,916.0	2,261.7	7.6	3,217.2	3,535.9	3,285.1	3,826.4	2,807.4		
			30	2.6	2,071.2	2,142.2	2,230.8	2,229.5	2,383.7	11.4	1,680.0	2,218.1	2,087.9	2,156.5	2,141.9		
Pulsar	17,898	8	18	11.1	6,271.4	1,011.7	953.0	1,131.5	3,817.7	43.1	5,574.6	919.4	1,042.3	1,226.1	3,595.0		
			20	19.6	2,920.8	470.3	485.5	531.0	1,820.1	81.0	3,114.9	338.7	345.5	481.6	1,686.8		
			25	21.5	2,473.3	300.4	265.8	373.2	1,990.1	85.0	2,748.9	367.1	302.3	447.7	1,859.1		
			30	24.3	1,740.2	293.5	281.6	292.8	1,587.0	114.1	1,842.1	269.9	226.1	239.4	1,448.1		
			35	26.7	1,450.3	248.8	210.6	217.1	1,227.4	101.7	1,675.4	278.7	2				

Dataset	N	D	K	Deviation [%]		cpu [s]			min/max ratio [%]		
				$W(\mathcal{C})$	ABA	METIS	ABA	METIS	ABA	METIS	
Abalone	4,177	10	4	43,608,225.6	-0.015	-0.033	0.012	0.05	0.44	100	99.81
			5	34,886,579.4	-0.012	-0.042	0.008	0.05	100	99.76	
			6	29,071,810.6	-0.025	-0.046	0.007	0.05	100	99.71	
			8	21,803,856.3	-0.066	-0.084	0.006	0.07	100	99.62	
			10	17,442,803.4	-0.037	-0.137	0.005	0.08	100	100.00	
			7	92,291,346.3	-0.051	-0.057	0.010	0.08	0.94	100	99.80
Facebook	7,050	13	8	80,755,313.2	-0.074	-0.072	0.009	0.09	100	99.77	
			10	64,603,775.2	-0.101	-0.105	0.009	0.10	100	100.00	
			13	49,695,725.5	-0.115	-0.137	0.009	0.14	100	99.63	
			18	35,891,488.1	-0.156	-0.184	0.009	0.15	100	100.00	
			8	142,342,153.4	-0.062	-0.023	0.010	0.09	1.16	100	99.78
			10	113,873,814.6	-0.061	-0.029	0.009	0.09	100	99.72	
Frogs	7,195	22	13	87,595,159.2	-0.084	-0.038	0.009	0.13	100	99.64	
			15	75,915,782.8	-0.102	-0.051	0.009	0.13	100	100.00	
			16	71,170,863.4	-0.106	-0.048	0.010	0.13	100	100.00	
			10	119,987,955.2	-0.055	-0.081	0.012	0.15	1.52	100	99.70
			15	79,991,945.9	-0.071	-0.135	0.011	0.17	100	99.70	
			20	59,993,929.0	-0.086	-0.189	0.012	0.22	100	100.00	
Electric	10,000	12	25	47,995,120.7	-0.109	-0.251	0.012	0.18	100	100.00	
			30	39,995,930.0	-0.131	-0.294	0.014	0.26	100	99.40	
			2	454,941,914.0	-0.006	-0.012	0.041	0.09	3.02	100	99.81
			4	227,470,912.0	-0.020	-0.028	0.022	0.13	100	99.85	
			6	151,647,232.0	-0.026	-0.039	0.016	0.12	100	99.89	
			18	142,364,702.5	-0.051	-0.077	0.023	0.35	3.04	100	99.80
Pulsar	17,898	8	20	128,128,230.1	-0.033	-0.095	0.023	0.37	100	99.78	
			25	102,502,571.6	-0.058	-0.117	0.027	0.39	100	100.00	
			30	85,418,864.6	-0.101	-0.146	0.029	0.53	100	99.66	
			35	73,216,081.5	-0.110	-0.160	0.034	0.55	100	99.61	
			2	10,799,639,983.1	-0.002	-0.004	0.112	0.30	12.37	100	99.80
			4	5,399,819,967.1	-0.005	-0.008	0.061	0.39	100	99.83	
Adult	32,561	110	6	3,599,879,960.7	-0.004	-0.015	0.046	0.48	100	99.78	
			2	58,310,221,872.3	-0.002	-0.003	0.136	0.34	74.02	100	99.80
			4	29,155,053,309.4	-0.008	-0.008	0.081	0.47	100	99.79	
			6	19,436,672,667.5	-0.016	-0.015	0.066	0.49	100	99.82	
			2	4,488,688,357.0	-0.002	-0.003	0.139	0.37	37.43	100	99.80
			4	2,244,344,114.0	-0.004	-0.009	0.078	0.46	100	99.86	
Plants	34,781	70	6	1,496,229,353.0	-0.006	-0.012	0.061	0.56	100	99.81	
			2	4,488,688,357.0	-0.002	-0.003	0.139	0.37	37.43	100	99.80
			4	2,244,344,114.0	-0.004	-0.009	0.078	0.46	100	99.86	
			6	1,496,229,353.0	-0.006	-0.012	0.061	0.56	100	99.81	
			2	54,165,709,163.4	-0.001	-0.001	0.182	0.53	50.43	100	99.79
			4	27,082,860,372.6	-0.004	-0.004	0.101	0.67	100	99.79	
Bank	45,211	53	6	18,055,235,145.3	-0.008	-0.007	0.075	0.80	100	99.79	
			Average		-0.050	-0.070	0.039	0.27	18.44	100	99.80

ABA is the contribution in this paper

Table 11: Comparing solution quality and running times of ABA, METIS, and random (Rand).

METIS. Once the representation of the dataset is constructed, the METIS algorithm can be used for different values of the number of anticlusters (K). Another drawback of the METIS software is that it requires integer edge weights. Because of this limitation, we rounded up non-integer weights. We applied METIS with its default settings. We used the datasets and the values for the number of anticlusters from Croella et al. [2025] and added five larger datasets, for which we tested $K = \{2, 4, 6\}$. Random partitioning (Rand) was again used as a baseline.

Table 11 reports the results. The first four columns list the name of the dataset, the number of objects (N), the number of features (D), and the number of anticlusters (K). Column 5 reports the within-anticluster sum of squared distances ($W(\mathcal{C})$) of the ABA algorithm. Columns 6 and 7 show the percentage deviation of the $W(\mathcal{C})$ values obtained by the benchmark algorithms from that of ABA. A negative deviation indicates an outperformance of the ABA algorithm. Columns 8 and 9 give the running time of the ABA algorithm and METIS, respectively in seconds. Column 9 lists for each dataset the running time required to construct the input for METIS, i.e., the construction of the adjacency list. Columns 10 and 11 report the ratio of the number of objects in the smallest anticluster to that in the largest anticluster for the ABA algorithm and METIS, respectively. This ratio should be one, except when the total number of objects (N) is not divisible by the number of anticlusters (K). In such cases, if the difference in size between the largest and smallest anticluster is at most one, we still report the ratio as 1.

Table 11 shows that ABA consistently outperforms METIS in both solution quality and speed. This outperformance tends to increase with increasing values of K . Moreover, as shown in columns 10 and 11, the ABA algorithm always produces perfectly balanced anticlusters, whereas METIS does not always achieve this. Both the ABA algorithm and METIS outperform Rand in terms of solution quality.

6 Conclusions

In this paper, we present a novel heuristic algorithm called Assignment-Based Anticlustering (ABA) for solving large-scale Euclidean anticlustering problems. The ABA algorithm iteratively assigns batches of objects to anticlusters by solving assignment problems. Two methodological contributions make our approach efficient and effective. First, we form the object batches based on each object's distance to the global centroid of the dataset, ensuring that objects with similar distances are in the same batch. This in turn ensures that all anticlusters have a similar diversity. Second, we represent the anticlusters by their centroids and thus can compute distances between objects and centroids rather than between pairs of objects. This reduces computational complexity and memory require-

ments. To further improve scalability, we propose a hierarchical decomposition strategy that recursively partitions anticlusters into smaller anticlusters. The hierarchical decomposition strategy enables the ABA algorithm to efficiently handle very large datasets with millions of objects and hundreds of thousands of anticlusters. We also show that the ABA algorithm can be extended to account for anticlustering with categories and can be applied to balanced cut and balanced k -cut problems on tabular Euclidean data. In a computational study on real-world datasets, we demonstrate that ABA consistently outperforms state-of-the-art heuristics in both solution quality and running time, often by large margins, especially when the number of anticlusters is large. Moreover, ABA produces anticlusters with more balanced diversity than existing methods.

Promising directions for future research include integrating approximate assignment solvers for example those that implement the Auction algorithm (see Bertsekas 1979). We also plan to develop a variant of the ABA algorithm for single anticluster problems such as the maximum diversity problem (MDP, see Hochbaum et al. 2023).

References

Kenneth R Baker and Stephen G Powell. Methods for assigning students to groups: A study of alternative objective functions. *Journal of the Operational Research Society*, 53(4):397–404, 2002.

Subhankar Banerjee and Shayok Chakraborty. Deterministic mini-batch sequencing for training deep neural networks. In *Proceedings of the AAAI Conference on Artificial Intelligence*, volume 35, pages 6723–6731, 2021.

Philipp Baumann, Olivier Goldschmidt, and Dorit S. Hochbaum. A fast algorithm for euclidean maximum weight non-bipartite matching. In *Proceedings of the 15th International Conference on Pattern Recognition Applications and Methods*, 2026. To appear.

Dimitri P Bertsekas. A distributed algorithm for the assignment problem. *Lab. for Information and Decision Systems Working Paper, MIT*, 3, 1979.

Michael J Brusco, J Dennis Cradit, and Douglas Steinley. Combining diversity and dispersion criteria for anticlustering: A bicriterion approach. *British Journal of Mathematical and Statistical Psychology*, 73(3):375–396, 2020.

Chao-Chiang Chen. *Placement and Partitioning Methods for Integrated Circuits Layout*. PhD thesis, EECS Department, University of California, Berkeley, 1986.

Anna Livia Croella, Veronica Piccialli, and Antonio M Sudoso. Strong bounds for large-scale minimum sum-of-squares clustering. *arXiv preprint arXiv:2502.08397*, 2025.

Thomas Feo, Olivier Goldschmidt, and Mallek Khellaf. One-half approximation algorithms for the k -partition problem. *Operations Research*, 40(1-supplement-1):S170–S173, 1992.

Thomas A Feo and Mallek Khellaf. A class of bounded approximation algorithms for graph partitioning. *Networks*, 20(2):181–195, 1990.

Micael Gallego, Manuel Laguna, Rafael Martí, and Abraham Duarte. Tabu search with strategic oscillation for the maximally diverse grouping problem. *Journal of the Operational Research Society*, 64(5):724–734, 2013.

Michael R. Garey and David S. Johnson. *Computers and Intractability; A Guide to the Theory of NP-Completeness*. W. H. Freeman & Co., USA, 1990. ISBN 0716710455.

Martin Grötschel and Yoshiko Wakabayashi. A cutting plane algorithm for a clustering problem. *Mathematical Programming*, 45(1):59–96, 1989.

Dorit S Hochbaum, Zhihao Liu, and Olivier Goldschmidt. A breakpoints based method for the maximum diversity and dispersion problems. In *SIAM Conference on Applied and Computational Discrete Algorithms (ACDA23)*, pages 189–200. SIAM, 2023.

KJ Joseph, Krishnakant Singh, Vineeth N Balasubramanian, et al. Submodular batch selection for training deep neural networks. *arXiv preprint arXiv:1906.08771*, 2019.

George Karypis and Vipin Kumar. A fast and high quality multilevel scheme for partitioning irregular graphs. *SIAM Journal on scientific Computing*, 20(1):359–392, 1998.

J Kral. To the problem of segmentation of a program. *Information Processing Machines*, 2(1):116–127, 1965.

Dmitry Krass and Anton Ovchinnikov. The university of toronto’s rotman school of management uses management science to create mba study groups. *Interfaces*, 36(2):126–137, 2006.

Xiangjing Lai and Jin-Kao Hao. Iterated maxima search for the maximally diverse grouping problem. *European Journal of Operational Research*, 254(3):780–800, 2016.

Xiangjing Lai, Jin-Kao Hao, Zhang-Hua Fu, and Dong Yue. Neighborhood decomposition based variable neighborhood search and tabu search for maximally diverse grouping. *European Journal of Operational Research*, 289(3):1067–1086, 2021.

Lara Mauri, Bruno Apolloni, and Ernesto Damiani. Robust ml model ensembles via risk-driven anti-clustering of training data. *Information Sciences*, 633:122–140, 2023.

Gintaras Palubeckis, Armantas Ostreika, and Dalius Rubliauskas. Maximally diverse grouping: an iterated tabu search approach. *Journal of the Operational Research Society*, 66(4):579–592, 2015.

Martin Papenberg. K-plus anticlustering: An improved k-means criterion for maximizing between-group similarity. *British Journal of Mathematical and Statistical Psychology*, 77(1):80–102, 2024.

Martin Papenberg and Gunnar W Klau. Using anticlustering to partition data sets into equivalent parts. *Psychological Methods*, 26(2):161, 2021.

Martin Papenberg, Martin Breuer, Max Diekhoff, Nguyen K Tran, and Gunnar W Klau. Extending the bicriterion approach for anticlustering: Exact and hybrid approaches. *Psychometrika*, pages 1–43, 2025a.

Martin Papenberg, Cheng Wang, Maïgane Diop, Syed Hassan Bukhari, Boris Oskotsky, Brittany R Davidson, Kim Chi Vo, Binya Liu, Juan C Irwin, Alexis J Combes, et al. Anticlustering for sample allocation to minimize batch effects. *Cell Reports Methods*, 5(8), 2025b.

Arne Schulz. The balanced maximally diverse grouping problem with block constraints. *European Journal of Operational Research*, 294(1):42–53, 2021.

Arne Schulz. A new mixed-integer programming formulation for the maximally diverse grouping problem with attribute values. *Annals of Operations Research*, 318(1):501–530, 2022.

Arne Schulz. The balanced maximally diverse grouping problem with integer attribute values. *Journal of Combinatorial Optimization*, 45(5):135, 2023a.

Arne Schulz. The balanced maximally diverse grouping problem with attribute values. *Discrete Applied Mathematics*, 335:82–103, 2023b.

Kavita Singh and Shyam Sundar. A new hybrid genetic algorithm for the maximally diverse grouping problem. *International Journal of Machine Learning and Cybernetics*, 10(10):2921–2940, 2019.

H. Späth. Anticlustering: maximizing the variance criterion. *Control and Cybernetics*, 15:213–218, 1986.

Shengjie Wang, Wenruo Bai, Chandrashekhar Lavania, and Jeff Bilmes. Fixing mini-batch sequences with hierarchical robust partitioning. In *The 22nd International Conference on Artificial Intelligence and Statistics*, pages 3352–3361. PMLR, 2019.

RR Weitz and S Lakshminarayanan. An empirical comparison of heuristic and graph theoretic methods for creating maximally diverse groups, vlsi design, and exam scheduling. *Omega*, 25(4):473–482, 1997.

Xiao Yang, Zonghui Cai, Ting Jin, Zheng Tang, and Shangce Gao. A three-phase search approach with dynamic population size for solving the maximally diverse grouping problem. *European Journal of Operational Research*, 302(3):925–953, 2022.

7 Appendix

Below we provide the proof of Fact 1.

Proof. Fix an anticluster \mathcal{C}_k of size $n_k = |\mathcal{C}_k|$, and let its centroid be

$$\boldsymbol{\mu}_k = \frac{1}{n_k} \sum_{i \in \mathcal{C}_k} \mathbf{x}_i.$$

We start with

$$\sum_{i, i' \in \mathcal{C}_k, i < i'} \|\mathbf{x}_i - \mathbf{x}_{i'}\|_2^2.$$

Expanding the squared norm gives

$$\|\mathbf{x}_i - \mathbf{x}_{i'}\|_2^2 = \|\mathbf{x}_i\|_2^2 + \|\mathbf{x}_{i'}\|_2^2 - 2 \mathbf{x}_i^\top \mathbf{x}_{i'}.$$

Hence,

$$\sum_{i, i' \in \mathcal{C}_k, i < i'} \|\mathbf{x}_i - \mathbf{x}_{i'}\|_2^2 = (n_k - 1) \sum_{i \in \mathcal{C}_k} \|\mathbf{x}_i\|_2^2 - 2 \sum_{i, i' \in \mathcal{C}_k, i < i'} \mathbf{x}_i^\top \mathbf{x}_{i'}.$$

Using

$$\left\| \sum_{i \in \mathcal{C}_k} \mathbf{x}_i \right\|_2^2 = \sum_{i \in \mathcal{C}_k} \|\mathbf{x}_i\|_2^2 + 2 \sum_{i, i' \in \mathcal{C}_k, i < i'} \mathbf{x}_i^\top \mathbf{x}_{i'},$$

we can express the cross term as

$$2 \sum_{i, i' \in \mathcal{C}_k, i < i'} \mathbf{x}_i^\top \mathbf{x}_{i'} = \left\| \sum_{i \in \mathcal{C}_k} \mathbf{x}_i \right\|_2^2 - \sum_{i \in \mathcal{C}_k} \|\mathbf{x}_i\|_2^2.$$

Substituting this into the previous equation yields

$$\sum_{i, i' \in \mathcal{C}_k, i < i'} \|\mathbf{x}_i - \mathbf{x}_{i'}\|_2^2 = n_k \sum_{i \in \mathcal{C}_k} \|\mathbf{x}_i\|_2^2 - \left\| \sum_{i \in \mathcal{C}_k} \mathbf{x}_i \right\|_2^2.$$

Since $\sum_{i \in \mathcal{C}_k} \mathbf{x}_i = n_k \boldsymbol{\mu}_k$, this becomes

$$\sum_{i, i' \in \mathcal{C}_k, i < i'} \|\mathbf{x}_i - \mathbf{x}_{i'}\|_2^2 = n_k \sum_{i \in \mathcal{C}_k} \|\mathbf{x}_i\|_2^2 - n_k^2 \|\boldsymbol{\mu}_k\|_2^2.$$

Finally, expanding

$$n_k \sum_{i \in \mathcal{C}_k} \|\mathbf{x}_i - \boldsymbol{\mu}_k\|_2^2 = n_k \sum_{i \in \mathcal{C}_k} (\|\mathbf{x}_i\|_2^2 - 2 \mathbf{x}_i^\top \boldsymbol{\mu}_k + \|\boldsymbol{\mu}_k\|_2^2) = n_k \sum_{i \in \mathcal{C}_k} \|\mathbf{x}_i\|_2^2 - n_k^2 \|\boldsymbol{\mu}_k\|_2^2,$$

we see both sides coincide. Therefore,

$$\sum_{i, i' \in \mathcal{C}_k, i < i'} \|\mathbf{x}_i - \mathbf{x}_{i'}\|_2^2 = n_k \sum_{i \in \mathcal{C}_k} \|\mathbf{x}_i - \boldsymbol{\mu}_k\|_2^2.$$

□